

ITT INDUSTRIAL LABORATORIES

A DIVISION OF INTERNATIONAL TELEPHONE AND TELEGRAPH CORPORATION
3700 East Pontiac Street • Fort Wayne 1, Indiana

November 23, 1966

NASA Headquarters
Washington, D. C. 20546

Attention: Code SCA

Subject : Contract NASW-1038
Second Phase Final Report

Reference: INTIL Project 11-21200

Gentlemen:

Enclosed are ten (10) copies and reproducible mats of the Second Phase Final Report as called for by the subject contract, Item B, Article V. The report and transmittal letter have been directly distributed, in accordance with your instruction, to the offices shown below.

Very truly yours,

ITT INDUSTRIAL LABORATORIES DIVISION

ORIGINAL
SIGNED BY

J. E. RALPH **167 13106**

John E. Ralph
Sr. Contract Administrator

JER:rr
Encs.

cc: (Report and Letter): Above address, Code SCA (1)
Above address, Code ATF (1)
Scientific & Technical Information
Facility (2)
P. O. Box 33
College Park, Md. 20740
Attn: SAMUEL

(Letter only):

DCISO, Ft. Wayne, Indiana
Attn: Mr. W. W. Lynch
Attn: Production Division

FINAL REPORT

RESEARCH IN THE DEVELOPMENT OF

AN IMPROVED MULTIPLIER PHOTOTUBE

Contract NASw 1038

F. H. Barr and E. H. Eberhardt

International Telephone and Telegraph Corporation
Industrial Laboratories Division
3700 East Pontiac Street
Fort Wayne, Indiana

November 16, 1966

GPO PRICE \$ _____

CFSTI PRICE(S) \$ _____

Hard copy (HC) 3.00

Microfiche (MF) 1.75



ff 653 July 65

National Aeronautics and Space Administration Headquarters
Washington, D. C. 20546

N 67 13106
(ACCESSION NUMBER)
78
(PAGES)
CR-80475
(NASA CR OR TMX OR AD NUMBER)

(THRU)
/ (CODE)
09
(CATEGORY)

ITTIL No. 66-1058

FINAL REPORT

RESEARCH IN THE DEVELOPMENT OF
AN IMPROVED MULTIPLIER PHOTOTUBE

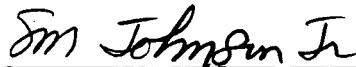
Contract NASw 1038

F. H. Barr and E. H. Eberhardt

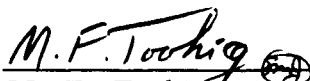
International Telephone and Telegraph Corporation
Industrial Laboratories Division
3700 East Pontiac Street
Fort Wayne, Indiana

November 16, 1966


Approved by



S. M. Johnson, Jr., Manager
Advanced Product Development



M. F. Toohig, Manager
Tubes and Sensors Department



Dr. C. W. Steeg, Director
Product Development

TABLE OF CONTENTS

		Page
1.0	INTRODUCTION-----	1
2.0	CASCADE APERTURE DESIGN -----	3
2.1	Aperture Separate From Dynode One -----	3
2.2	Aperture Mounted on Dynode One -----	5
3.0	RESIDUAL GAS PRESSURE EFFECTS -----	15
4.0	GAIN CALIBRATION-----	19
5.0	COOLING TESTS -----	20
5.1	Equipment Description and Modifications -----	20
5.2	Cooling Test Data -----	22
6.0	VARIABLE EFFECTIVE PHOTOCATHODE AREA -----	33
7.0	HIGH QUANTUM EFFICIENCY, MULTI-PASS CATHODES ---	35
8.0	LARGE EFFECTIVE PHOTOCATHODE AREA -----	41
8.1	Cathode Characteristics -----	43
8.2	Multiplier Response Time Characteristics -----	43
8.3	Pulse Amplitude Distribution Characteristics -----	47
9.0	MULTIELECTRON PULSE INVESTIGATION -----	59
10.0	SECONDARY ELECTRON DEFLECTION AT DYNODE ONE --	64
	APPENDIX I APPLICATIONS NOTE E4 COOLING CHARACTERISTICS OF ITTIL MULTIPLIER PHOTOTUBES -----	70

1.0 INTRODUCTION

This report covers the work performed during the second year's effort on NASw 1038. It covers a number of basic problems and innovations in the design of multiplier phototubes for single event counting. These basic problems are as follows:

1. An evolution and summary of the data on the "cascade operation" design as a method of controlling low energy electrons in the region of the defining aperture and dynode one. This is an important region since improper functioning at this point can degrade the statistics of the multiplier so as to render it incapable of counting applications. A new dynode one design is also briefly evaluated.
2. The dark noise characteristics of certain photocathode type multipliers have been investigated by cathode cooling techniques. While it is understood that NASA does not have a prime interest in this method of operation, notwithstanding NASA users who operate in this mode exclusively, it constitutes a powerful investigative technique.
3. An investigation of the counting properties of tubes in which the instantaneous effective cathode diameter (IEPD) has been increased by a new tube design to approximately 0.4 inch to 0.5 inch. These investigations have been undertaken because of the information received as a result of our numerous contacts with astronomical observatories including Lick, Yerkes, Washburn, McDonald and Sydney (Australia) Observatories, which have indicated an urgent need for counting photomultiplier tubes of this type.
4. An investigation of the counting properties and increased effective photon counting efficiencies of tubes especially designed for enhancement of the cathode quantum efficiency by means of "multi-bounce" optical techniques. It is clear that improved optical detectors will require a combination of the highest possible cathode quantum efficiency and the best electron counting capabilities, and we have attempted to optimize these properties by incorporating a rectangular effective cathode area (encompassing the multi-bounce areas) in one of our electron counting tubes.

5. Measurements of pulse response properties of counting tubes. This investigation was instigated because of the expressed need for fast response by astronomers in order to cover as wide a dynamic counting rate range as possible without modifying the detector system, a desirable objective in extracting the maximum amount of stellar information.
6. An investigation of multi-electron pulses was undertaken as a remedial step toward correcting a problem encountered in a new tube design. The results are quite conclusive though other problems need further study.

2.0 CASCADE APERTURE DESIGN

The preliminary work on this modification of the defining aperture, dynode one region, was reported in the second quarterly report of the first year of this project. This modification consists of the insertion of a second or "cascade", aperture of somewhat larger diameter between the defining aperture and dynode one with a lead brought out through the wall of the glass envelope, so that its potential may be independently controlled. It was suggested that a simplification of the design could be achieved by mounting this aperture on dynode one, thus eliminating this extra lead. Varying the potential of this combined electrode with respect to the defining aperture should then give the same degree of control as with the aperture separate. While this is a simplification for the user, it results in a complication during assembly of the multiplier tube. This situation arises from the fact that the two subassemblies, the image section and the electron multiplier, are finally joined in the glass envelope by sliding the electron multiplier up behind the defining aperture plate so that a flat index pin engages a slot in the aperture plate to reference the two assemblies with respect to each other. However, this technique does not assure that the aperture on dynode one will be accurately aligned with the defining aperture since the indexing pin is located off axis on the multiplier assembly and it is possible for the two sections of the tube to rotate with respect to each other during final seal-in, thus allowing one aperture to move from its desired location directly below the other. In the case of the separate aperture, the alignment can be more easily performed by mounting the cascade aperture off the defining aperture plate before this assembly is inserted into the envelope. While these problems are, in general, simply a matter of designing the appropriate assembly jigs and fixtures, they are mentioned here as a possible reason for the rather wide variation in the optimum operating potential for the cascade aperture or the aperture-dynode one combination. It is not known how much the hand assembly techniques have affected these operating parameters, but it seems reasonable to assume that tighter control on the geometry of this critical region would result in more uniform characteristics. The following data is presented as evidence that the aperture mounted in dynode one is as effective, in producing good single electron spectra as was the separate aperture tube reported earlier. Data on two tubes with separate apertures is also given.

2.1 Aperture Separate From Dynode One

Figure 1 is a schematic representation of the electrode configuration and applied potentials for this set of data. The following plots are a series of spectra taken with individual tubes. The figure above each spectra is the potential of the cascade aperture with respect to the defining aperture. In the interest of conserving time and space the spectra was compressed into the first 30 channels of the 100 channel analyzer which accounts for the periodic or folded abscissa scale. These plots also represent a departure from the way the data was recorded in previous reports in that the signal spectra do not have the dark spectra subtracted out. This accounts for the rapidly rising characteristic seen in the early channels.

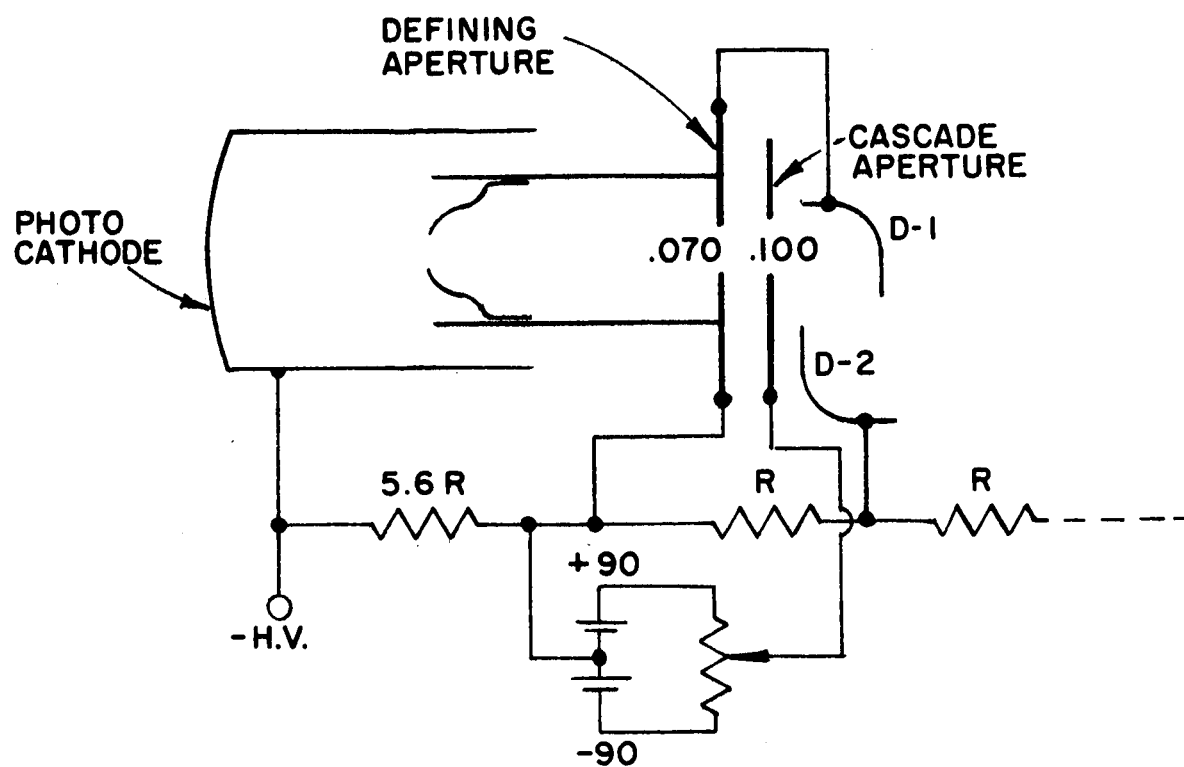


Figure 1

It can be seen, however, that if the dark spectra (exponential curve) was subtracted, the signal spectra would show a marked reduction of low amplitude pulses.

Figure 2 is a series of spectra with the cascade aperture varied from +20 to -40 volts with respect to the defining aperture. In this series, the total dark count is relatively constant from -10 to -40 volts, but at 0 and 20 volts, there is an increasing number of small pulses with higher negative potential applied to the cascade aperture. The signal spectrum is without a valley until -20 volts at which point a peak-to-valley ratio of 1.2 is obtained. This condition seems to be optimum for this tube notwithstanding the fact that the total dark count is somewhat more than 1000 counts per 0.1 minute higher than at -10 volts.

Figure 3 shows a tube with similar characteristics but over a considerably wider range of aperture voltages. The optimum cascade aperture potential is about -60 volts giving a peak-to-valley ratio of 1.25. There is some tendency for the total dark count to decrease with more negative potential, but the dark counting rate is so high in the early channels that one might logically attribute some of it to noise sources external to the tube.

There is, however, one operating parameter, namely the potential of dynode two, which was optimized for these spectra. It was found that +56 volts on dynode two, with respect to dynode one, optimized the output pulse amplitude. This voltage is about half of the nominal dynode-to-dynode voltage and is also in good agreement with the recently discovered operating conditions for minimum output signal shading of this type of multiplier phototube, when used in applications where the surface of dynode one is scanned by the image of a point source of light focused on the photocathode. Whether or not there exists a relation between this mode of operation and optimum conditions for single electron counting applications has yet to be determined. Since output signal shading is an indication of non-uniform collection efficiency, however, the optimization of this parameter should aid in preventing the loss of counts between dynodes one and two.

2.2 Aperture Mounted on Dynode One

Figure 4 is, again, a schematic diagram of the operating conditions when the aperture is mounted directly on dynode one. This, of course, requires that the potential of dynode one change as well as that of the aperture while dynode two remains fixed with respect to the defining aperture.

Figure 5 shows a series of spectra in which the peak begins to occur at -10 volts with the optimum conditions at -60 volts at which point a peak-to-valley ratio of 1.6 is obtained. Dark counts are responsible for majority of the rapidly rising number of small pulses and there is little tendency for these counts to diminish with more negative voltage on dynode one. A change in gain also accompanies the change in aperture-dynode one potential as indicated by the broadening distribution.

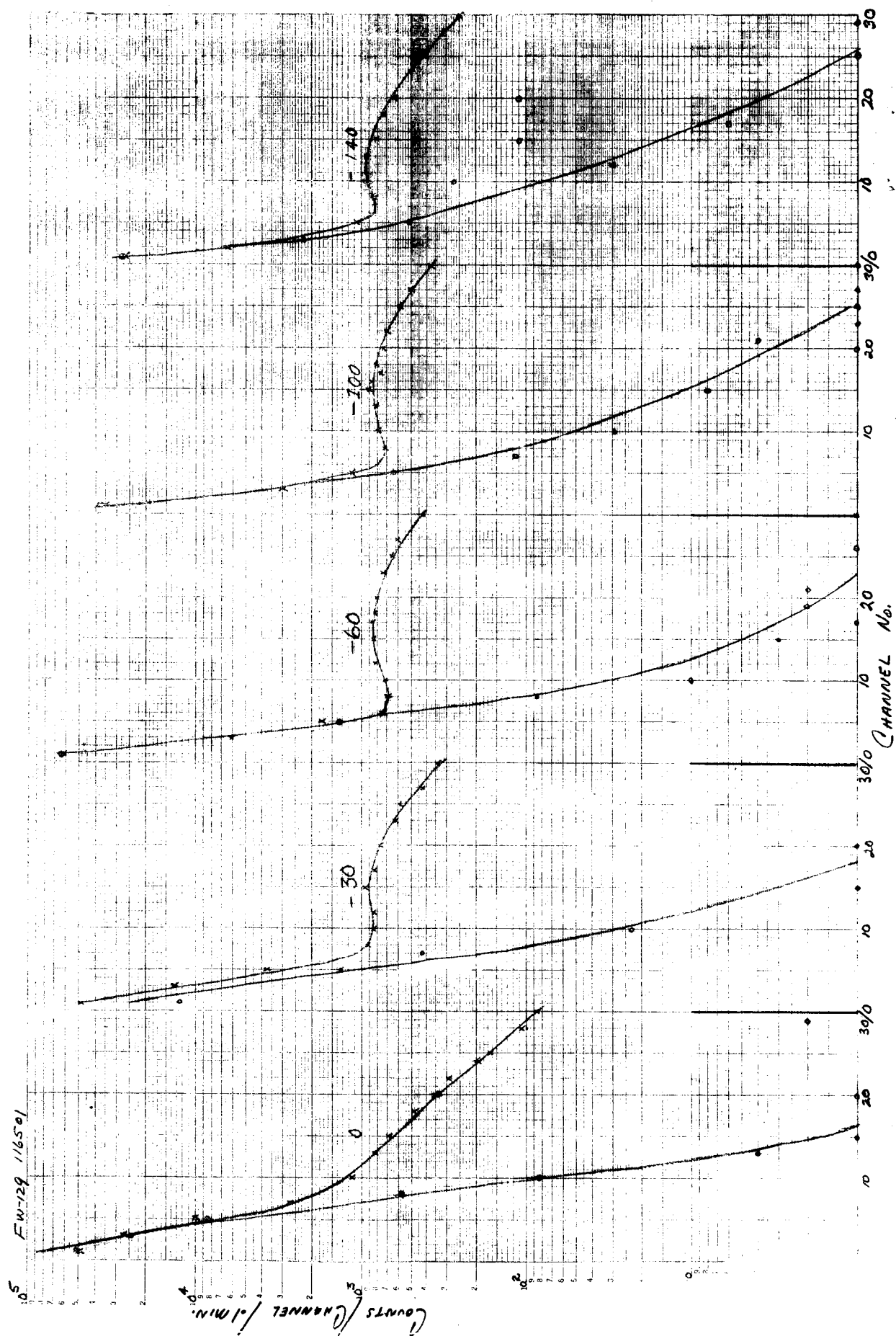


Figure 3

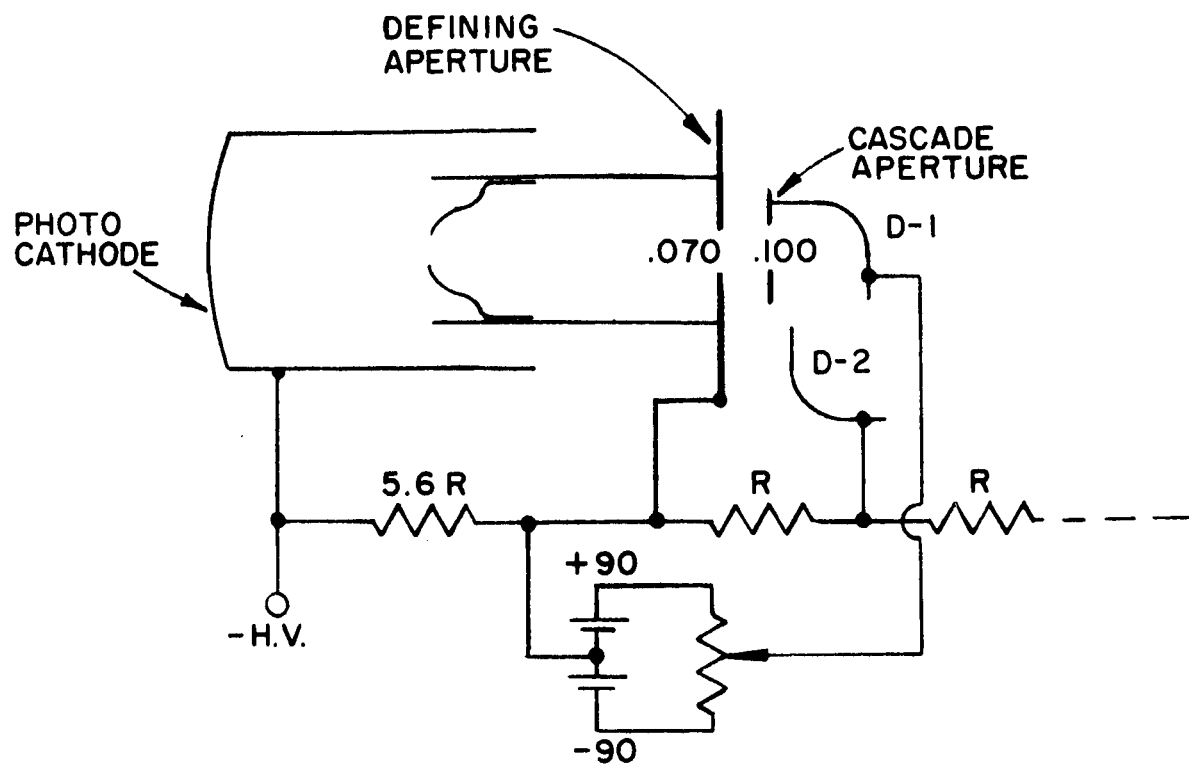


Figure 6

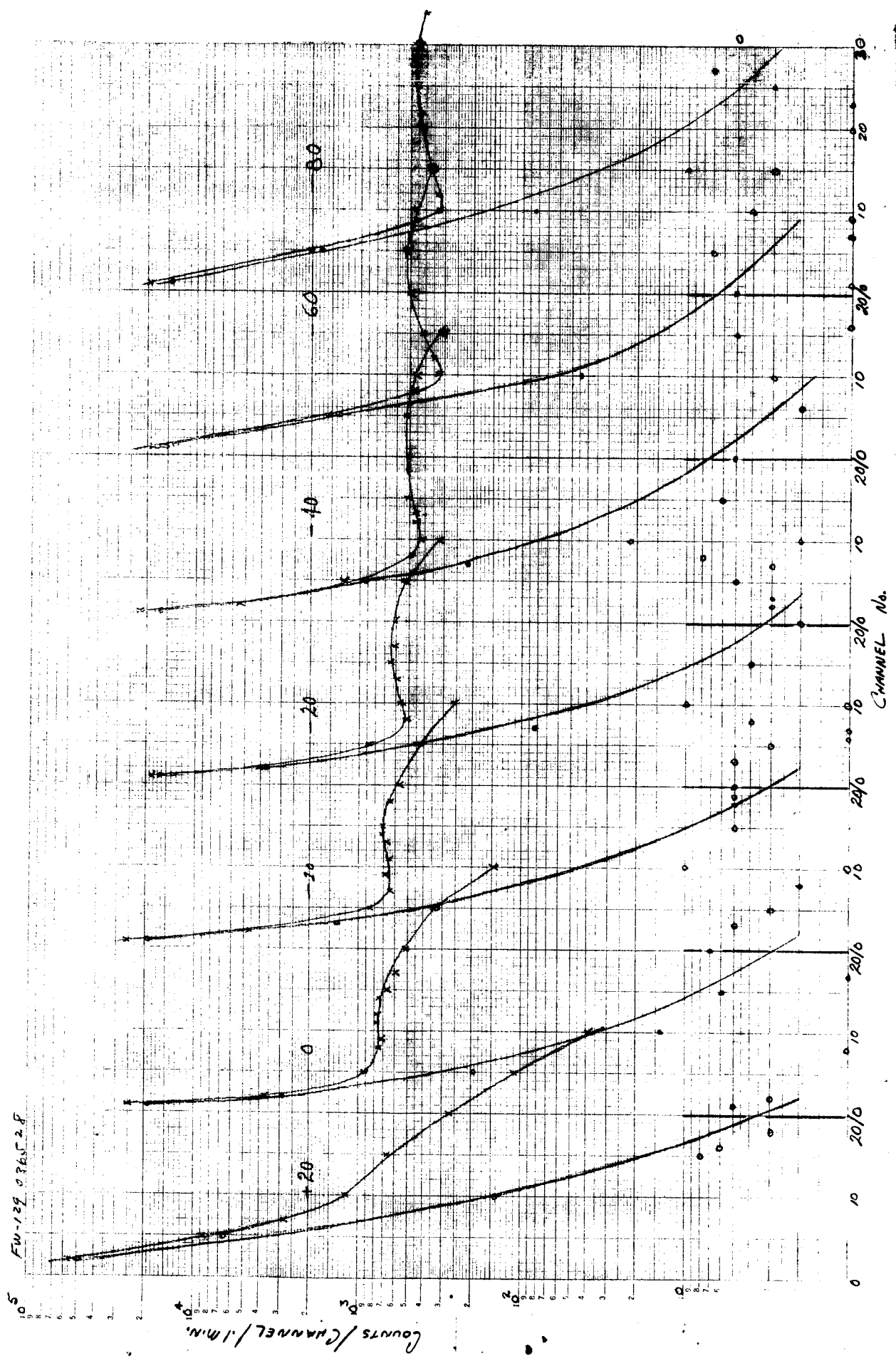


Figure 5

Figures 6 and 7 are the test results of two tubes that seem to have superior characteristics compared to the others that have been reported. In Figure 6, there is a dramatic drop (of greater than an order of magnitude!) in the dark count at zero volts on the aperture-dynode one electrode, and a distinct valley in the distribution occurs around channel five. A -20 volts produces the best peak-to-valley ratio in this case with a value of 1.35.

In Figure 7 there is again a great reduction in the dark count at zero volts, but instead of decreasing further or remaining constant, there is a slight rise in the count. It is interesting to note, however, that in this tube the dark count, at any given aperture-dynode one voltage, drops off much more rapidly than it does for the previous tubes. A peak-to-valley ratio of 1.8 occurs for 0 to -20 volts although this ratio does not change appreciably even at -60 volts. A gain change, however, seems to follow this voltage change which, of course, tends to broaden the spectrum.

Table I is a summary of the data just presented with some additional characteristics which are calculated from it. The table is self-explanatory except perhaps for the two counting efficiencies.

If one considers the application of these tubes to counting circuits, it is obvious that a bias level or threshold must be established corresponding to the smallest pulse which is to be accepted. This then eliminates the smaller than average pulses which make up the exponentially rising portion of the spectrum. Because of the statistical nature of the multiplication process in the tube, it will be impossible to set this bias so that only dark pulses are biased off while at the same time allowing all signal pulses to be counted, therefore some signal pulses will be lost. In Table I it is assumed, for the purpose of computing the counting efficiency, that this bias would be set at the valley channel tabulated. Now the Minimum Counting Efficiency is defined as the ratio of the total signal counts, C_{TS} , minus the signal counts lost, C_{LS} , due to the bias setting, to the total signal counts.

$$\text{Counting Efficiency} = \frac{C_{TS} - C_{LS}}{C_{TS}}$$

The Extrapolated Counting Efficiency is obtained by projecting the signal spectrum from the tabulated valley channel back to channel zero, as would be predicted by true Poissonian, statistics, and computing the above ratio again.

The gain figures in this table were arrived at in a manner unique to the pulse counting mode of operation and will be discussed later in the report.

It seems apparent that the cascade aperture design as applied to the ITTIL line of multiplier phototubes provides a distinct improvement in the single electron response of these tubes. In all cases, Figures 2, 3, 5, 6 and 7, a distinct improvement in the peak-to-valley ratio was observed experimentally for optimum settings of the decelerating electric field between the two apertures. It should be pointed out

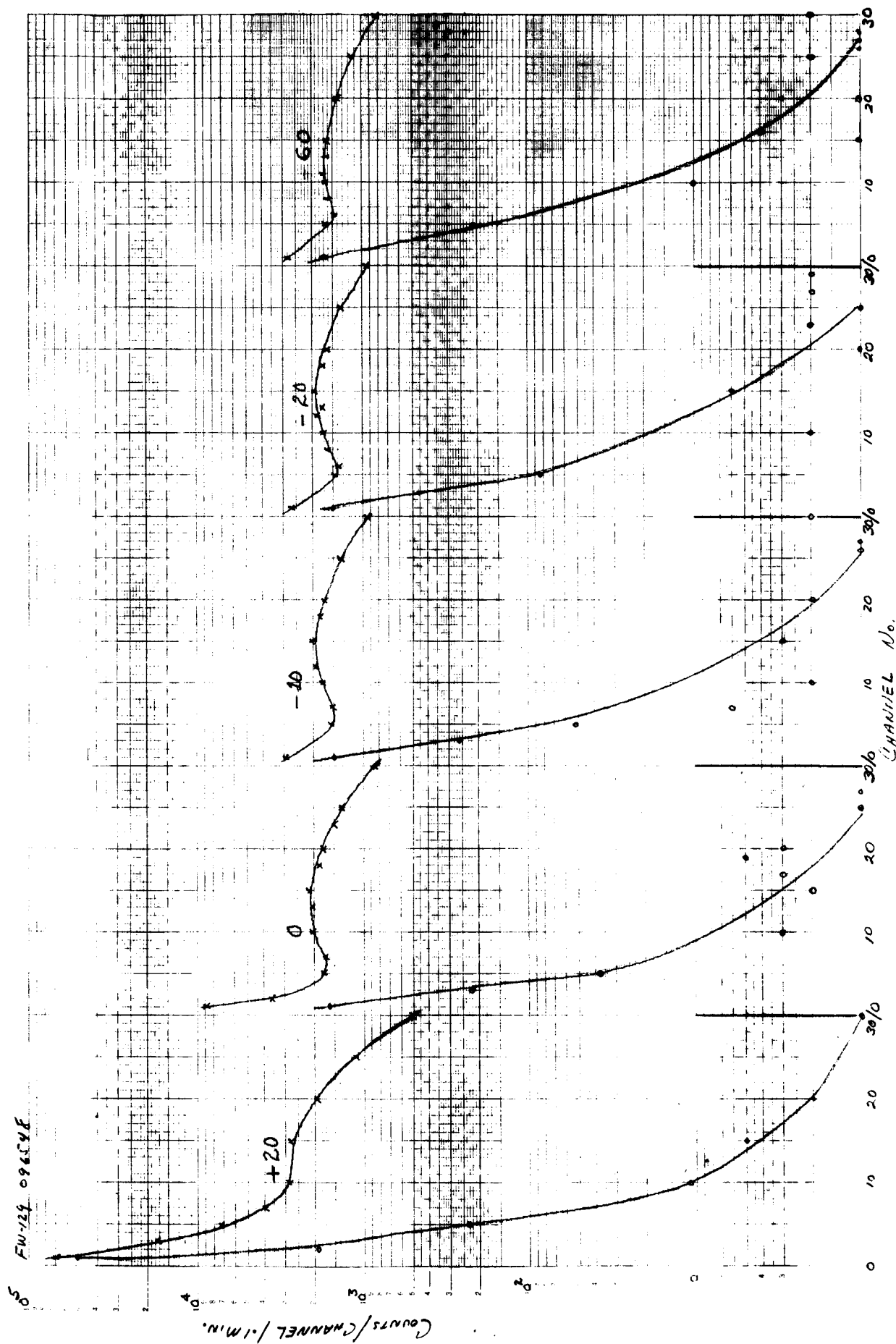


Figure 6

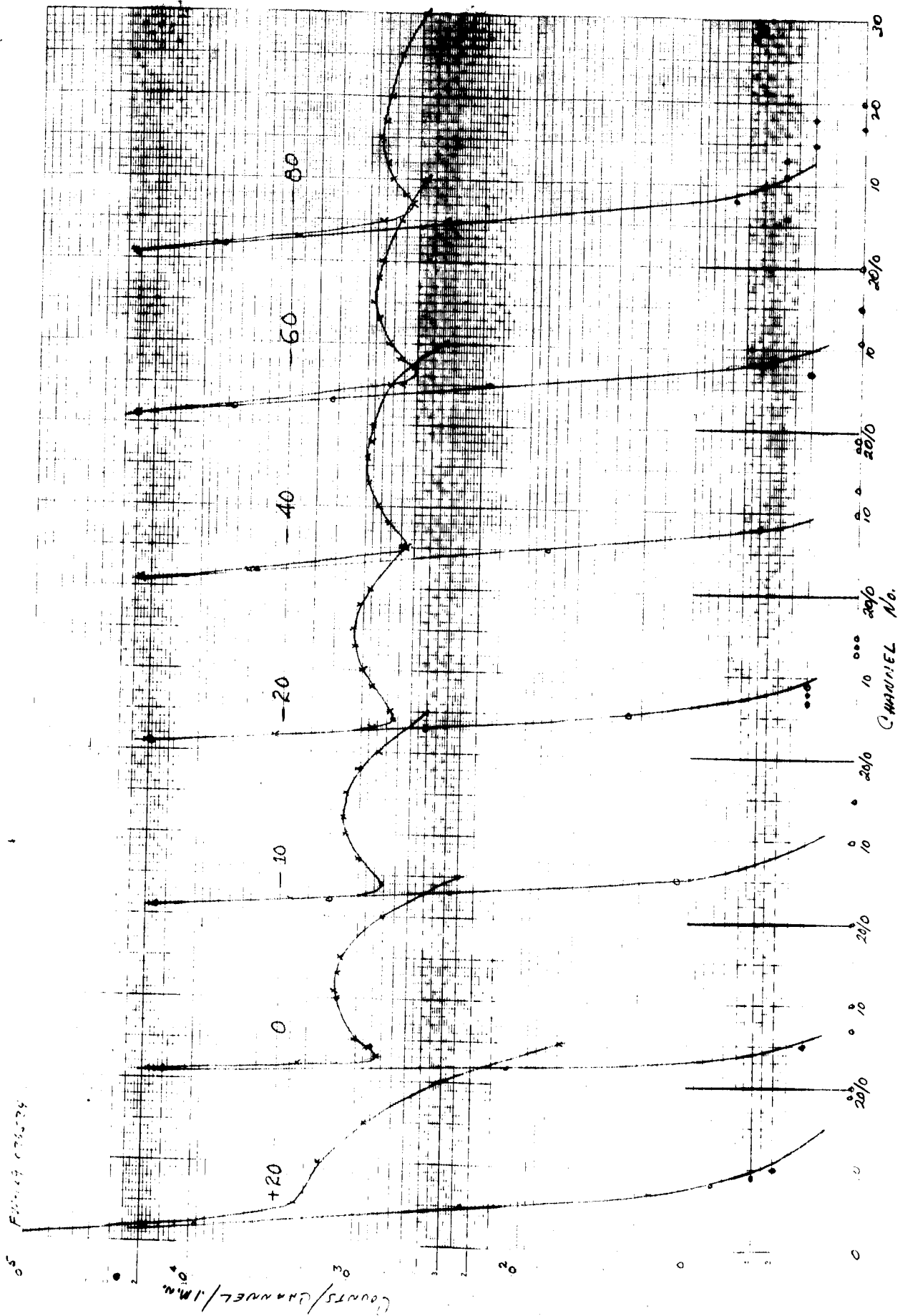


Figure 7

Table I

Tube Number	Operating Voltage	Gain	Optimum Cascade Aperture Potential (Volts)	Peak-To-Valley Ratio	Valley Channel Number	Minimum Counting Efficiency (%)	Extrapolated Counting Efficiency (%)	Total Dark Counts/Sec. Above Valley Channel
126463	1800	1.9×10^6	-20	1.2:1	7	76	86	200
116501	1600	6.3×10^5	-60	1.25:1	8	88	91	311
036528	1800	4.7×10^5	-60	1.6:1	10	77	91	64
096548	1800	3.1×10^5	-20	1.35:1	6	86	90	16
036534	1700	1×10^6	-10	1.8:1	4	91	95	25

that the tubes tested were all of the S-11 type, of standard construction with 0.7 magnification electron optics and 0.140 inch effective photocathode diameter. In view of the above data, it seems wise to recommend that the cascade aperture design be applied to future multiplier tubes which are specifically intended for use as single event counters.

3.0 RESIDUAL GAS PRESSURE EFFECTS

During this present investigation, we have noticed on the triggered oscilloscope display, which monitors the input to the analyzer, pulses which are much larger than the single electron pulses. These pulses are of such amplitude that on the normal scale of the single electron spectrum, they occur beyond the range of the analyzer display and so are not seen.

To determine what effect gas pressure and temperature have on these pulses, three tubes were made with Kovar tubulations for cold seal-off, thus reducing gas evolution as compared to hot glass seal-off techniques. One of these tubes have been tested and tipped off, another has had partial tests made on it, and has not been sealed off, while the third has not been tested. This tube had a Bayard-Alpert type ion gauge attached to it in the hope that more accurate pressure measurements could be made. Unfortunately, the particular gauge used is not compatible with the power supplies presently available, so that tests on this unit were temporarily deferred.

Figure 8 is the signal and dark spectra of this tube at pressures of 10^{-7} torr and 3×10^{-9} torr, which are the pressures after removal from the exhaust system and the pressure after ion pumping, respectively. There is no significant difference in the signal spectra and only a slight reduction in the dark count. Figure 9 is a group of these dark spectra taken with this tube in the region from channel 50 to 120. Since the analyzer is only capable of displaying 100 channels of information, it was necessary to offset the baseline of the instrument to display channels equivalent to 35 to 135 and move the threshold up to cut off the first 35 channels to save counting time. Because of the low counting rate in this portion of the spectrum, a total counting time of 30 minutes was required to accumulate a reasonable number of counts. The 24 degree C curve at 10^{-7} torr is the condition in which the tube came off the exhaust system, the ion pump being turned on just long enough to read this pressure. A nichrome ribbon heater was then wrapped around the base end of the tube on the glass envelope just above the Kovar weld ring and heated slowly to 130 degrees C at which point the pressure had risen to 5×10^{-6} torr. The data clearly indicates an increase in the number of these large pulses and the assumption is that it is due to gas evolution since the pressure has also increased. The two curves are about 100 to 150 counts apart between channels 70 and 90 where they indicate a broad band of preferred amplitudes between channels 75 and 80. Subsequently, the ion pump was operated until a pressure of 10^{-9} torr was attained. At this pressure, the ion pump was pinched off and the feather edge of the tubulation was soldered to protect it from damage during baseing. This tube was then retested at room temperature and the sharply falling 24 degree C 10^{-9} torr curve was obtained. A further indication of the pressure dependence of these multielectron pulses was demonstrated.

FW-129-096550

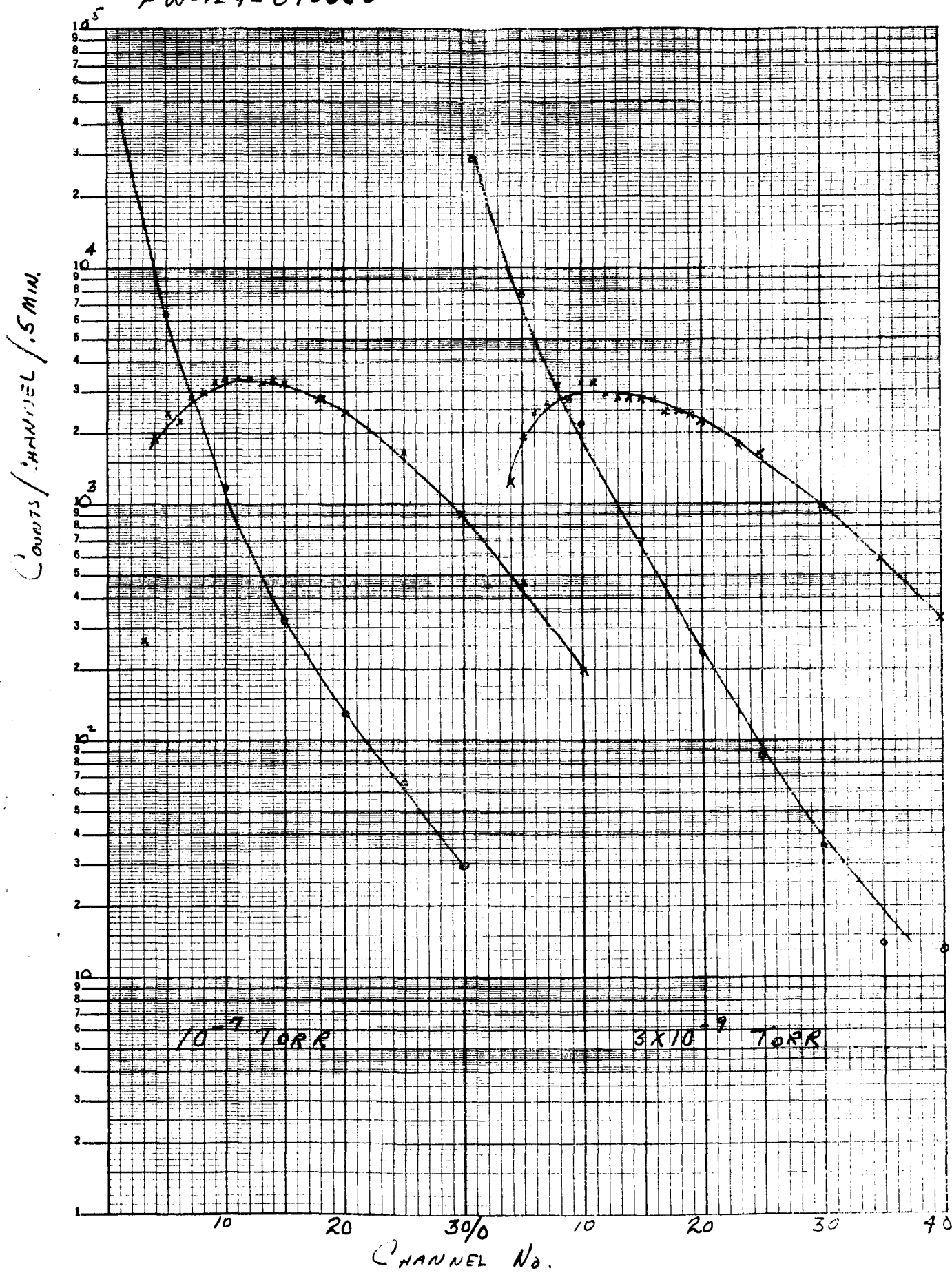
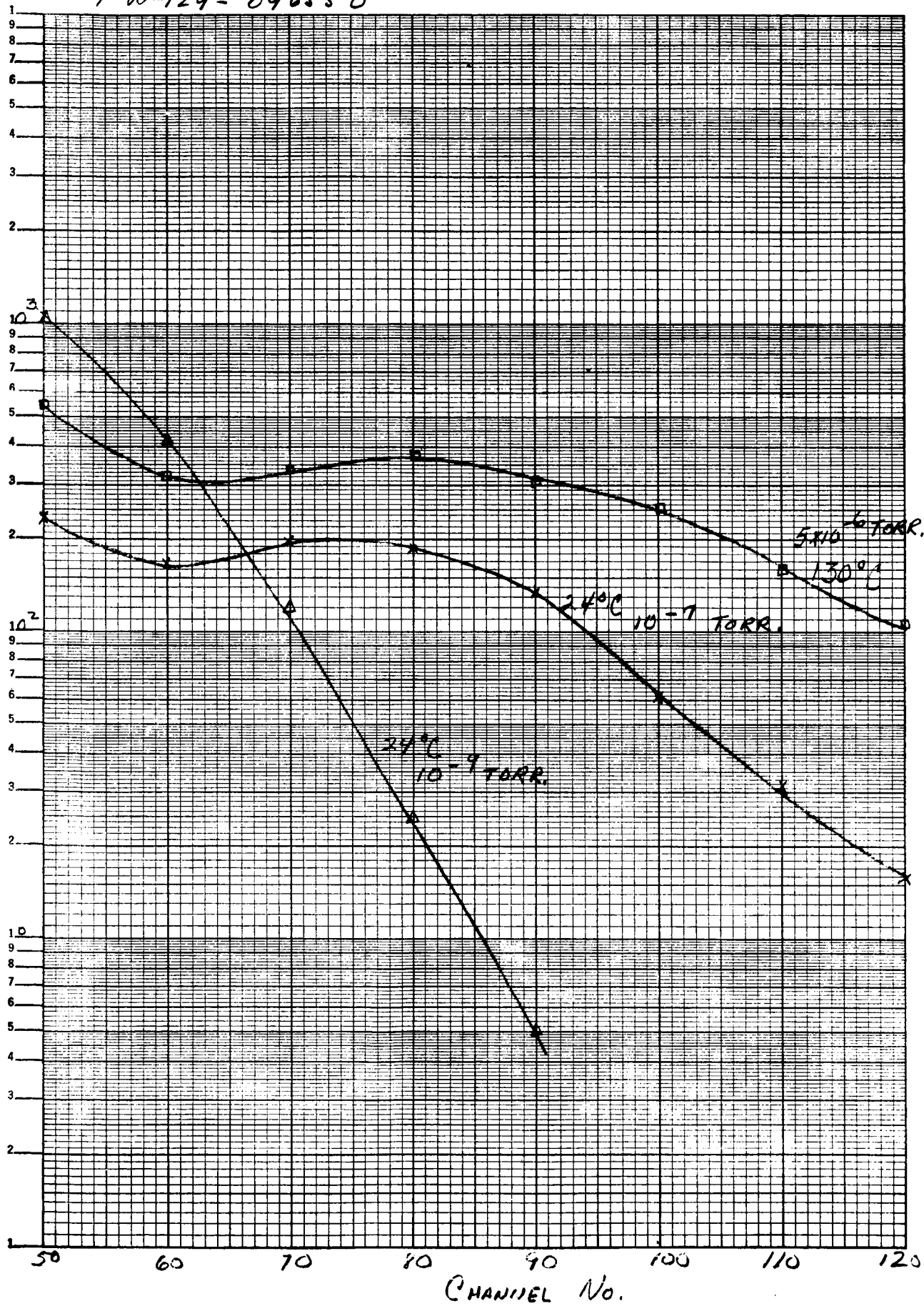


Figure 8

FW-129-096550

COUNTS / CHANNEL / 50 nD.



CHANNEL No.

Figure 9

In connection with this data, a preliminary calibration of this pulse amplifier analyzer combination was made, using an Ortec Model 204 Precision Pulse Generator. With this generator, a pulse of known amplitude is fed into the amplifier. This pulse is then stored in the appropriate channel of the analyzer memory according to its amplitude, as any other pulse would be. Since this amplitude is variable by means of a linear precision potentiometer, one can pick out any channel and determine the amplitude of a pulse that would fall in that channel for any given set of conditions established by the analyzer controls. In the case of the 3×10^{-9} torr curve of Figure 8, channel 10 was taken to be the most probable pulse amplitude and by the method described above is equivalent to 0.008 volt. At this point in the experiment, it had not been established definitely that the baseline and the threshold controls were linear and produced the 35 channel offset mentioned earlier. However, a pulse fed into the channel which should have been number 70, had indeed an amplitude of 0.054 volt. The ratio $0.054/0.008$ is very close to 7 indicating that channel 70 is equal to 7 electrons, channel 80 is 8 electrons, channel 90 is 9 electrons, etc. This evidence tends to support the belief of workers in this laboratory that gas ions, produced by the collision of electrons with residual gas molecules, are accelerated back to the cathode where they are effective in exciting multielectron pulses. A visual corollary to this situation, however, has frequently been observed in the case of an image converter using the same electron optics that are used in the image section of these multiplier tubes. As one looks at the output of the flooded gassy image converter tube, a bright spot is seen at the center of the phosphor screen. If the flooding light is blocked off the cathode, the bright spot disappears or is greatly diminished, indicating that the electrons exciting the phosphor were, in turn, produced by gas ions bombarding the photocathode, the ions being produced by bombardment of residual gas molecules by photoelectrons. (In a dark room one still observes a dim spot generated by ions produced by thermionic electrons.) If the light is blocked off just at the center of the cathode, the bright spot persists nearly undiminished. As the tube is operated, the spot gradually degenerates into a black spot and when the cathode sensitivity is locally investigated a serious loss in sensitivity due to ion bombardment is found at the center of the cathode. This damage to the cathode is greatly accelerated in the above case due to the higher current density as compared to the counting mode of operation.

Several attempts have been made to duplicate these results in tubes of this type but with attached Bayard Alpert gauges and side appendages for more careful control and monitoring of gas pressure as mentioned above. It was possible to vary the gas pressure by these means but no evidence was seen of a preferred multi-electron pulse amplitude as in the case of tube number 096550.

4.0 GAIN CALIBRATION

A knowledge of the average pulse amplitude makes possible another interesting calculation, namely, the gain of the multiplier. The total charge, Q , delivered, to the amplifier by the anode of the multiplier is given by the fundamental relationship.

$$Q = C \bar{v}$$

where C is the total capacity of the anode circuit which includes the amplifier input, and \bar{v} is the average pulse amplitude. The total anode circuit capacity is $8 \times 10^{-11} \mu\text{f}$ and average pulse amplitude is nominally 8×10^{-3} volts. This calculation yields a figure of 6.4×10^{-13} for the total charge, Q . Since this total charge, Q , is the product of the electronic charge, e and the gain of the multiplier we may write

$$\mu = \frac{Q}{e} = \frac{6.4 \times 10^{-13}}{1.6 \times 10^{-19}} = 4 \times 10^6$$

A measurement of the tube's cathode sensitivity gives $47 \mu\text{A}/\text{lumen}$ and the measured output of the tube, with the standard equipment in this laboratory, is $43 \text{ amperes}/\text{lumen}$ for the particular over-all voltage and voltage distribution. Calculating the gain again as the ratio of the output current to the input gives

$$\mu = \frac{43 \text{ A/L}}{4.7 \times 10^{-5} \text{ A/L}} = 9.2 \times 10^5$$

which is in fair agreement with the pulse method considering the possible error accumulation in the calibration of standard lamps (1 lumen and $0.1 \mu \text{ lumen}$) and associated instruments used to make these measurements. This means of gain calibration, as can be seen, requires only the knowledge of a measurable circuit constant, an established physical constant, and the average pulse amplitude which is obtained from the spectrum data being gathered. This method then is useful in maintaining a constant check on multiplier gain without the need for a standard source of illumination and associated equipment, assuming of course that the gain stability of the electronics can be maintained.

A more elegant method of calibrating the gain of the multiplier might be to use a monochromatic light source of known output energy and, therefore, known photon flux to excite the cathode. The equipment could then be calibrated in terms of electrons per pulse since the circuit capacity and pulse amplitude are known. By this method, the quantum efficiency of the cathode in terms of electrons per photon could be determined and the gain of the tube could be given in terms of electrons out per electron in.

5.0 COOLING TESTS

One of the primary uses of multiplier phototubes is in astronomical applications where high quantum efficiency and low noise are required for maximum information acquisition. Because it is usually desired to push the multiplier phototube to its fundamental limit of sensitivity, namely, counting charge pulses at its output, dark noise pulses must be reduced to a level where signal pulses can be counted with minimum ambiguity. Assuming that dark pulses are primarily due to thermionic emission in a well designed tube, it should then be possible to cool the photocathode to substantially reduce these pulses. For S-1 photocathodes, the thermionic emission characteristics are well known, and Richardson plots of the dark current versus temperature have been reported.¹ In the case, however, of the S-20 trialkali cathode, this information is not readily available. Since this type of cathode has a high visible sensitivity from 3500 Å to 8500 Å, it is useful to stellar spectrometry, and in certain laser applications where the available radiation may be quite small. For this reason, it was considered essential to investigate the cooled mode of operation of tubes with this cathode to determine what could be expected in terms of improved signal-to-noise ratio.

The technique used in this investigation was that of cooling the tube, particularly the photocathode. Because of the necessity for obtaining a low over-all noise level and the ability to monitor cathode temperatures, some time was required to adapt the cooling equipment toward this end. Different modes of multiplier operation were also tried to determine their effect on multiplier noise.

In addition, this report includes data on some tubes built on other projects. The results of these tests bear directly on the purpose of this project and so were considered to be basically an extension of this NASA research effort.

5.1 Equipment Description and Modifications

The multiplier phototube refrigerated chamber used in this work was a model TE-200 manufactured by Products for Research, Inc., of West Acton, Mass. This unit uses dry ice and alcohol as the coolant, and is capable of producing cathode temperatures of -68 degrees C in an ambient of 0 degrees C to +40 degrees C. It has a removable double plexiglass input window at one end and the other end of the chamber is fitted with an "O" ring sealed socket assembly in which the voltage divider may be potted. High voltage input and collector output connector are included on this assembly. Because of the versatility required of this equipment, the socket assembly was modified so that the dynode leads came out through a shielded cable and were terminated in a 20 pin tube base so it could be plugged into the standard test fixture. In addition to this, two teflon insulated wires and a chromel-alumel thermocouple were brought out through this assembly from the cold chamber so that control potentials could be applied to such special electrodes as the cascade aperture. This also allows the cathode temperature to be monitored. All leads through the socket assembly were potted in place to prevent air leakage and subsequent frosting.

While this cooler in general is quite satisfactory, there are two points where careful grounding are necessary to assure low noise performance. First, there must be a ground strap between the collector coaxial output connector, which is mounted in the side of the bakelite socket assembly, and the aluminum cover through which the shielded cable is brought out. This strap is necessary even though these two parts are grounded by way of the cable shields.

Secondly, it was discovered that the coolant tank around the multiplier tube is electrically floating as the cooler is supplied. After consulting the manufacturer, it was found possible to remove the front cover of the cooler, remove a small amount of the foam insulation surrounding the filling port and fasten a ground strap to it. This strap was brought out through a hole in the top of the case where it was fastened to a lug under one of the front plate mounting screws. The foam insulation removed during this procedure was then replaced.

A further source of difficulty was found with the pulse preamplifier-multi-channel analyzer combination. While these two instruments (Tennelec Model TC-M-170 preamplifier and TMC Model 101-100 channel analyzer) functioned properly in themselves, they were not compatible as they were received from the manufacturer due to pulse shape considerations. This incompatibility takes the form of nonlinearity in the last half of the memory, channels 50 to 100. On checking with the Tennelec Instrument Company, it was discovered that the preamplifier should have been modified, before delivery, so that the preamplifier output pulse shape matches the input requirements of the TMC-101 Analyzer. At the present time, the nuclear instrumentation industry is not standardized on the input pulse characteristics of multi-channel analyzers, but only on the input of the more expensive, high quality, linear amplifiers. This occurs because most users bypass the linear amplifiers in the analyzer and couple directly from an external linear amplifier into the analyzer ADC circuit. For this reason, prospective users of equipment similar to that used in this laboratory would be well advised to carefully check these considerations with the instrument supplier if they intend to purchase such equipment.

Our preamplifier has now been modified and the remaining non-linearity in the system is less than 2 percent. An additional improvement in the operation of the preamplifier (as a result of this modification) is the increased signal-to-noise ratio. Measured noise at the output of the preamplifier before modification was 5 mv; after modification, it was 2 to 2.5 mv. (This improvement was predicted by the manufacturer.)

As a result of these modifications, the over-all noise reduction has enabled us to count pulses of about half the amplitude as before without counting noise pulses which originate outside the tube.

5.2 Cooling Test Data

The cooling experiments were carried out in the following manner. With a tube enclosed in the cooler and all connections properly made, a dark current reading and a dark count were taken at room temperature. The temperature of the cathode was then reduced by filling the coolant tank. Actually, a somewhat more convenient method used was to blow dry nitrogen gas, cooled by liquid nitrogen, into the coolant tank. When a temperature of -60 degrees C was reached, the flow of the cold gas was reduced and the system allowed to come to equilibrium. The tube temperature was then raised by blowing warm air from a heat gun into the coolant chamber, and data was taken at 10 degree intervals, as the tube warmed up. Figures 10 and 11 are a series of curves showing the d-c dark current as a function of temperature for five tubes with S-20 cathodes. These tubes are standard pilot production tubes. The most obvious feature of these curves is the limited reduction in dark current due to cathode cooling. For S-1 cathodes it is not unreasonable to expect three to five orders of magnitude reduction in dark current for 50 degree C reduction in temperature. This data, however, fails to show similar results for S-20 cathodes. One exception was found in the case of F64-974-30 which is a special tube designed for wide dynamic range counting applications. The tube is constructed with the glass image section envelope connected to the metal multiplier section envelope by a heliarc weld ring. Aside from its unusual glass-metal envelope, it has an additional innovation in the collector stem lead. This lead is coaxial in design and comes out at the center of the stem. The anode itself is mounted on the center conductor in such a way as to be isolated from the photoceramic multiplier support members. This type of construction thereby eliminates possible leakage across the multiplier supports and may provide better isolation of the anode lead through the stem as well as more effective shielding from stray pickup noise. It would seem, then, from this assumption that in the case of the other tubes, the dark current curves bottom out on some d-c leakage level set by the condition of the glass stem and the ceramic multiplier support members. However, some of the standard tubes come within half an order of magnitude of the characteristics of this special tube.

A summary of the pertinent data is included with some calculated parameters in Table II. The first seven columns are self-explanatory. Column eight is the measured d-c anode dark current for the two extreme temperatures (+20 degrees C and -60 degrees C) for the curves in Figures 10 and 11. In column nine is recorded the corresponding photocathode dark count density which was taken at the same time the dark current was read. In column ten is the equivalent dark current density based on this dark count density for comparison with the dark current density based on d-c measurements. Column eleven is the dark current referenced to the cathode using the average d-c gain figures in column three and the cathode area in column six.

A comparison of the data in column eight and ten shows immediately the wide difference in the measured dark current density and the equivalent dark current density which implies that the dark current, on cooling, flattens off at the d-c leakage

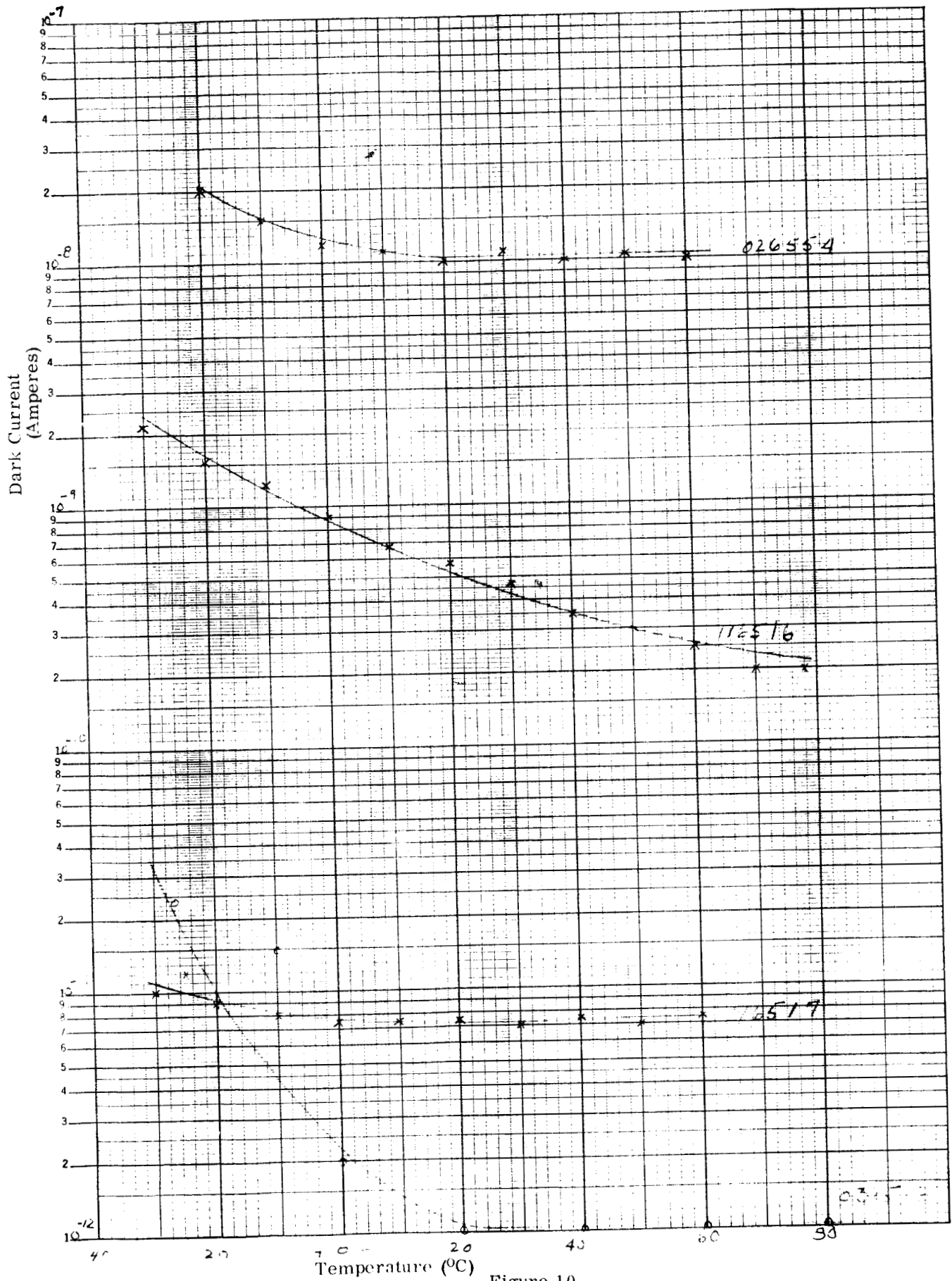


Figure 10

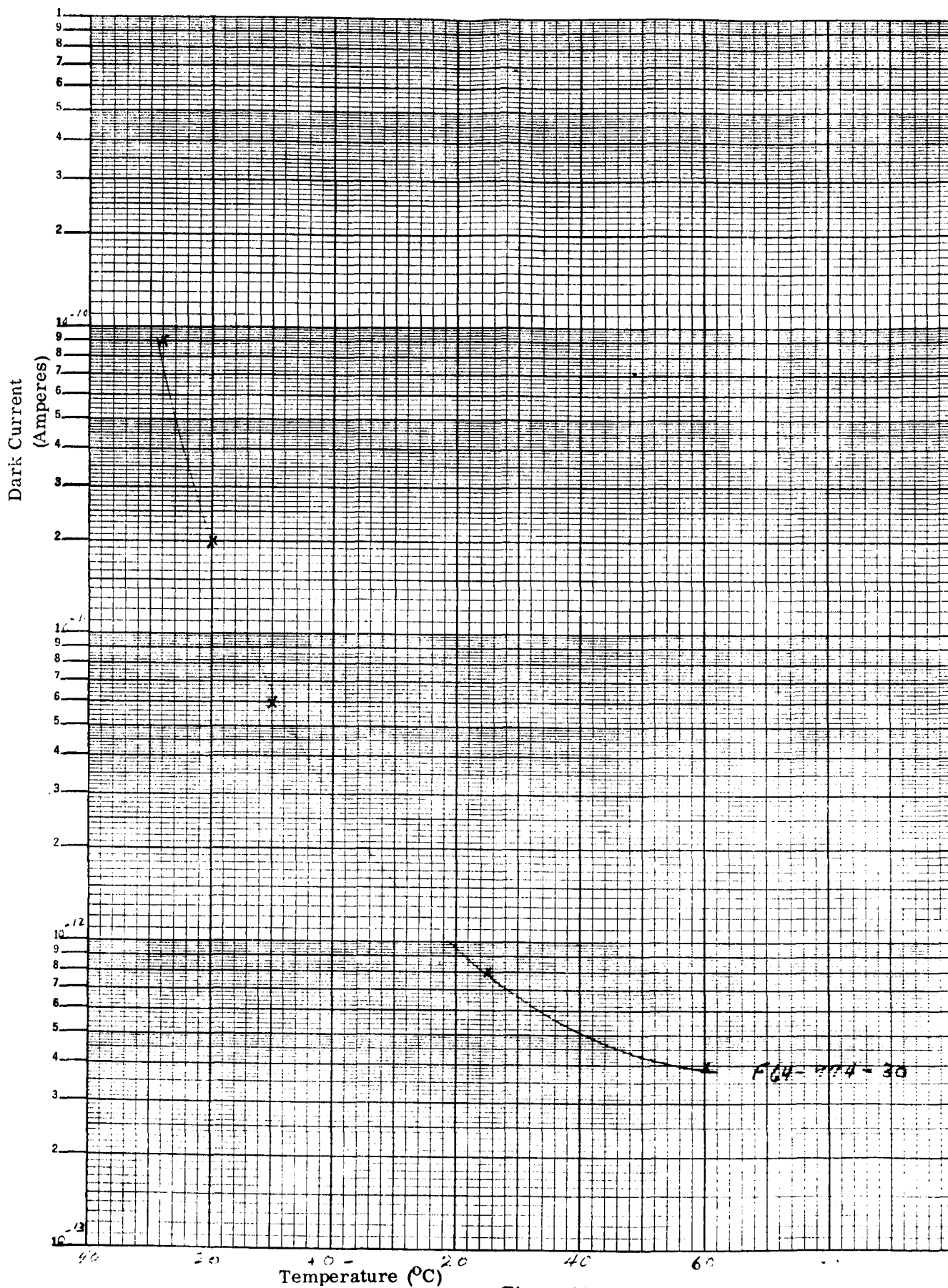


Figure 11

Table II

1	2	3	4	5	6	7	8	9	10	11
Tube Number	Operating Voltage	Average d-c Gain	Cathode Sens. ($\mu\text{a./l}$)		Cathode Area (Cm^2)	Cathode Temp. ($^{\circ}\text{C}$)	Measured d-c Anode Dark Current (Amperes)	Photocathode Dark Counts Per Cm^2 Per Second	Equivalent Photocathode Dark Current Density (Amps/ Cm^2)	Photocathode Dark Current Density (Amps/ Cm^2)
116517	1800	1.2×10^6	2870 $^{\circ}\text{K}$ Tungsten	Corning 2030 Filter	.62	20	1.0×10^{-11}	561	8.9×10^{-17}	1.3×10^{-17}
				12		-60	7.5×10^{-12}	10	1.6×10^{-18}	1×10^{-17}
116516	1800	2×10^6	105	10	.62	20	2.2×10^{-9}	8920	1.4×10^{-15}	1.8×10^{-15}
						-78	2.0×10^{-10}	827	1.3×10^{-16}	1.6×10^{-16}
026554	1800	3.6×10^6	100	20	.62	20	3.0×10^{-8}	1080	1.7×10^{-16}	1.3×10^{-14}
						-60	1.0×10^{-8}	387	6.2×10^{-17}	4.5×10^{-15}
036516	1800	8×10^5	98	16	1.27	20	6.5×10^{-12}	157	2.5×10^{-17}	6.4×10^{-18}
						-60	1.0×10^{-12}	9	1.4×10^{-18}	1×10^{-18}
F64-974-30 12 Stage Multiplier	2000	1.6×10^5	160	60	1.27	28	9.0×10^{-11}	2310	3.7×10^{-16}	4.4×10^{-16}
						-60	4.0×10^{-13}	Dark Count Obscured By Noise Pickup		2×10^{-18}

level. The same characteristic seems to be present in the dark count data for there is approximately the same reduction in dark count with cooling as in the case of dark current.

In checking the assumption made earlier, that the d-c anode dark current may be bottoming out at the d-c leakage level, it is of interest to compare the data in columns ten and eleven. In the case of tubes 116517, 116516, 036516, and F64-974-30 there is good agreement, within approximately an order of magnitude, between the equivalent dark current density and the cathode dark current density.

The differences in the data may be, at least in part, explained by the statistical nature of multiplication process for single events as compared to the average d-c methods of measuring gain. The agreement noted above, indeed, indicates that the dark current of these tubes on cooling does approach a limit that is essentially that of the cathode dark count density level and further that the room temperature thermionic emission level is only slightly higher. F64-974-30 is the exception to this for it has a sensitivity, in the spectral region beyond 7000 \AA , of 3 to 6 times that of the other tubes. This is not an unexpected result for one would expect such increased thermionic emission with increased red sensitivity, the S-1 cathode being a case in point. Tube number 026554 does not show the agreement between equivalent dark current density and cathode dark current density that the other tubes do. Both at room temperature and at -60 degrees C, the cathode dark current density is two orders of magnitude higher. Since the cathode dark current density is the d-c anode dark current referenced back to cathode, this difference is apparently d-c leakage in the anode circuit. This leakage, undesirable as it may be, does not seem to contribute to the dark count. As a result of this condition two orders of magnitude improvement in sensitivity was obtained by applying counting techniques, as opposed to d-c measurement, to the output circuit for this particular tube.

In trying to explain the behavior of tubes, e. g. number 026554, where cooling did not produce the expected dark current reduction, a problem that was given consideration was that of light generation by the phototube itself due to corona in the image section. For this purpose, a second multiplier with a very low dark counting rate was enclosed in a light-tight fixture and coupled to the window mounting ring of the cooling chamber. A dark spectrum was run for this tube with no voltage applied to the tube under test and following that a second count was taken, but with high voltage applied to the tube in the cooling chamber. No additional counts were recorded from the tube "looking" at the test tube even with an additional 400 or 500 volts applied to the tube being tested. Similar tests were made in a different enclosure so that the tube under test could be inspected in other areas, such as the aperture-dynode 1 region and the collector region. In no case was it possible to detect any kind of arcing or fluorescence which might be responsible for regenerative feedback to the photocathode. While such effects have been reported,² they were detected in tubes delivering high peak anode currents, and the glow produced was in the collector region of the tube.

Another problem area investigated was the effect of multiplier phototube ground point on the noise content. For many applications, the tube is operated with the cathode at high negative voltage and the anode at ground as shown in Figure 12 (a). For operation of the multiplier with the cathode at ground potential the modified divider is shown in Figure 12 (b). Since the high voltage signal coupling capacitor and decoupling network are supplied in the preamplifier itself, the only actual changes that had to be made were: (1) at the tube socket and (2) to shunt the 100-megohm resistor in the decoupling network with a 1 megohm resistor to maintain very nearly the same load impedance. The tube operation was quite satisfactory in this mode of operation, but it was discovered that when the cathode was connected to dynode 2, (i. e., biased off), as shown by the dashed arrow in Figure 12 (b), there still remained some large pulses, 3 to 5 times the amplitude of a single electron pulse, with a rate of about 300 or 400 per minute. This was quite different from the previous mode of operation, for in that case no pulses appeared in the output of the tube. Since the high voltage for the anode was applied through the preamplifier high voltage type BNC connector, it was suspected that signal input BNC connector of the low voltage type might be arcing to ground. When the preamplifier, however, was disconnected from the tube test fixture, the pulses stopped. On reconnecting the preamplifier to the test fixture and applying high voltage (but leaving the tube out of the socket), the pulses appeared again at the same rate. This indicated that the difficulty was arcing in the socket which was a Cinch Jones Type 20-PM cast of MAL-60 alkyd glass fiber material.

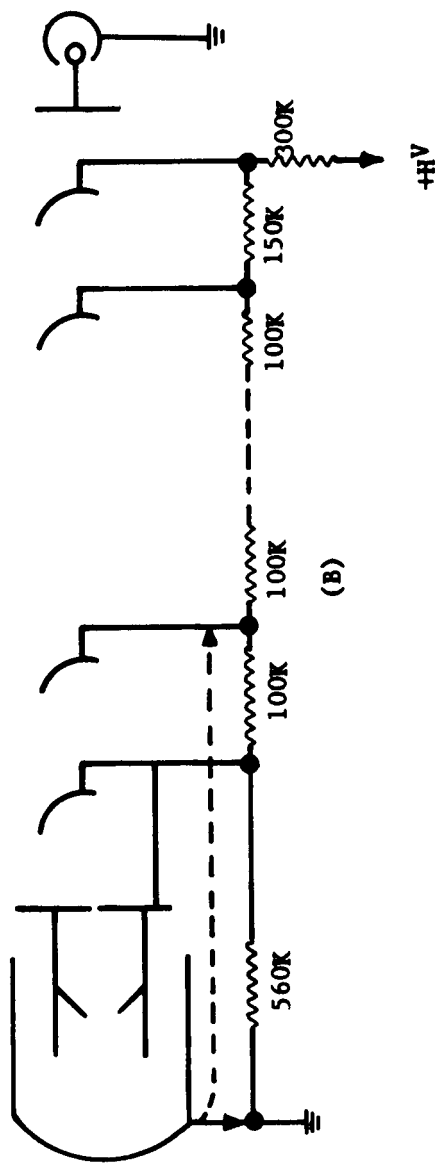
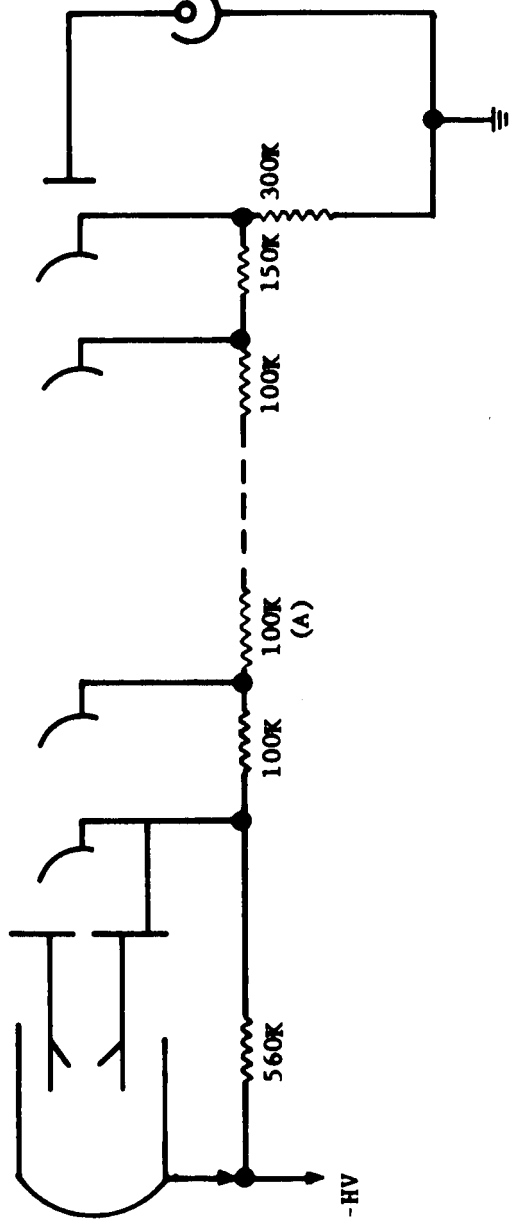
There did not seem to be any appreciable difference in these two modes of operation except for the noise introduced by arcing in the socket. The decision, therefore, as to grounding the cathode or anode of a multiplier phototube should be made on the basis of amplifier input coupling and insulation or other special conditions. If for any of these reasons, however, operation with anode at high positive potential is desirable, the user would be well advised to use another socket, if available, or to machine an appropriate socket out of teflon.

Figure 13 demonstrates one other aspect of the dark noise which has often been mentioned by multiplier phototube users, mainly the decay of the dark current or dark count with time. Out of the tubes tested, two showed a measurable effect.

The measurements were started immediately after the tube was placed in the dark enclosure and high voltage had not been applied to the tube while exposed to room level illumination. The data could be repeated simply by turning off the high voltage, lifting the dark enclosure cover, replacing the cover and again applying high voltage to the tube.

This would indicate that in low level counting applications, at least some tubes will require care in handling so that this situation does not render the data useless during the early minutes of operation.

MULTIPLIER PHOTOTUBE



PREAMP

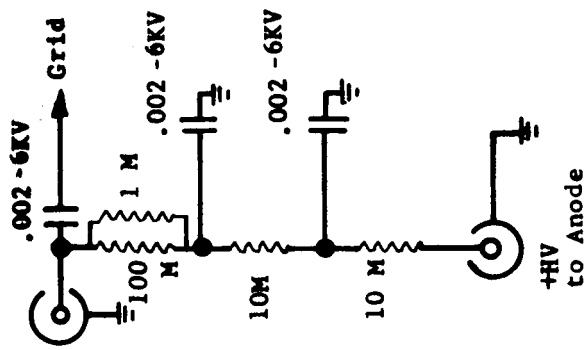
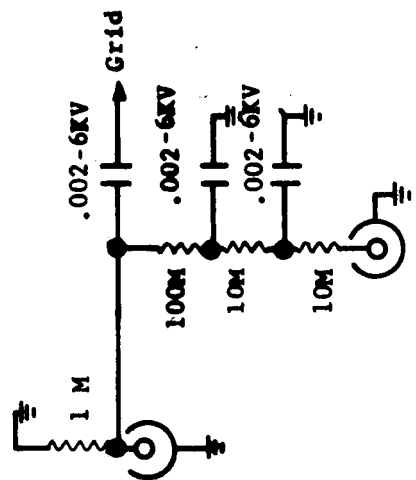


Figure 12

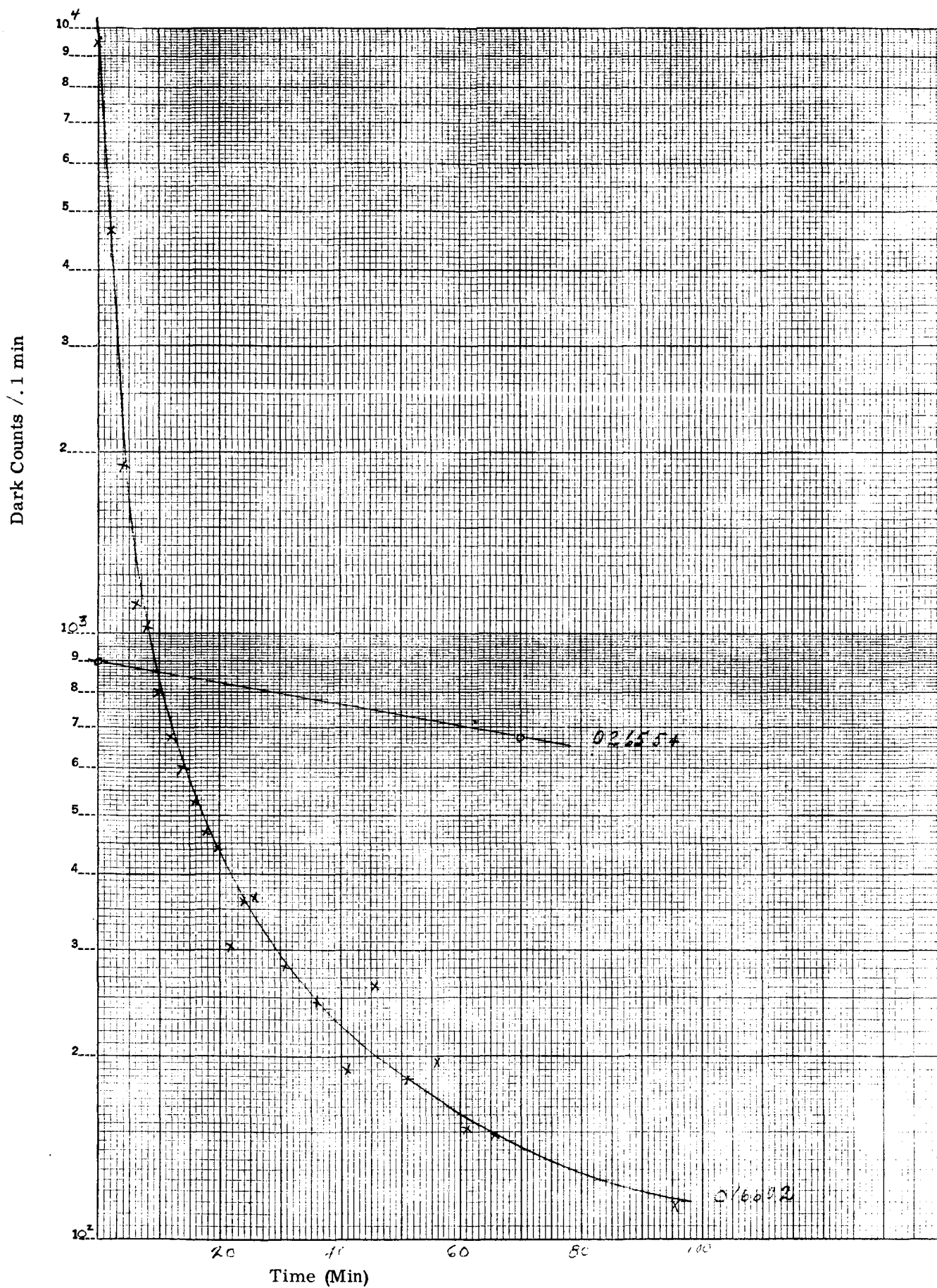


Figure 13

Before leaving the discussion of this group of tubes some data on the single electron counting capability of F64-970-30 should be discussed since it is the first of several tubes which represent a large scale modification of the standard ITTIL multiplier phototube design.

The tube is of 1 inch diameter glass tubing with the final seal made at the junction of the image section and multiplier section by a heliarc weld ring somewhat larger in diameter. The photocathode area has been enlarged by means of both aperture size and electron optical magnification adjustments.

The data in Figure 14 was taken on tube number F64-974-30, whose cooling characteristics were reported in the previous section of this report, with the cascade aperture at limiting aperture potential. The top curve is the total spectrum which included signal, thermionic, and dark emission. Note the absence of the rising characteristic in the early channels. This spectrum has a peak-to-valley ratio of 1.13.

The second curve is with the cathode illumination turned off so that only the thermionic and dark emission remain. Here a larger number of small pulses appear and there is no valley, but the general shape of the signal spectrum is maintained, undoubtedly because of the cathodes higher red sensitivity (16×10^{-3} A/W @ 7000 Å).

The dark spectrum is shown in the lower curve at a temperature of -60 degrees C. In the region of the peak of the signal spectrum, there are an average of only four counts per channel per tenth minute.

Figure 15 is data taken from the same tube, but with the cascade aperture at -45 volts with respect to the limiting aperture. The total spectrum has a somewhat better peak-to-valley ratio, 1.26, while the thermionic spectrum also has a peak, with a peak-to-valley ratio of 1.09. Inspection of the dark spectrum shows a significant change. Channels two and three have a reduction of more than 50 percent in the total counts per channel and there is an average of less than three counts per channel per tenth minute in the region of the peak.

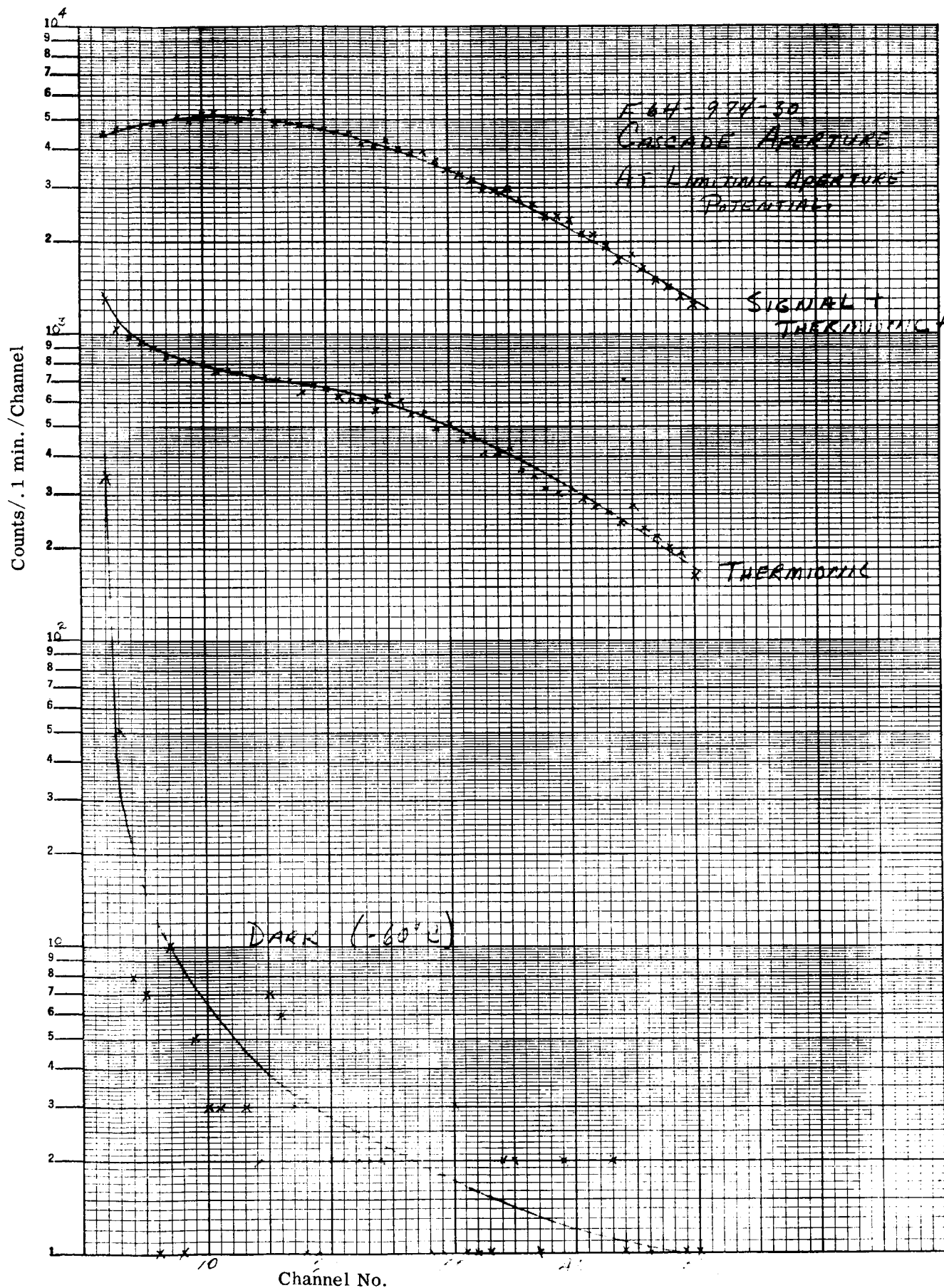


Figure 14

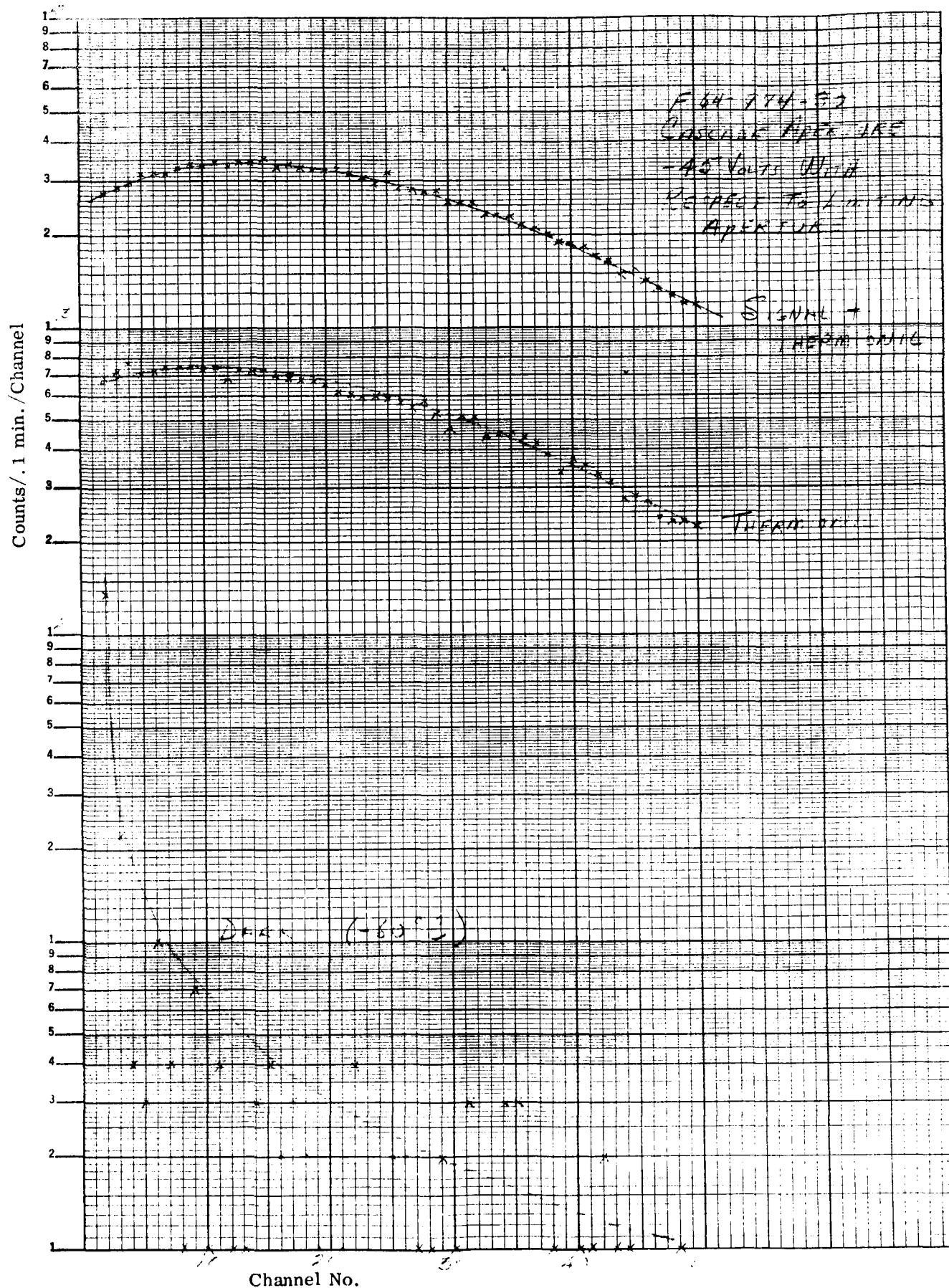


Figure 15

6.0 VARIABLE EFFECTIVE PHOTOCATHODE AREA

A recent innovation in the design of the aperture-to-dynode one area was made in a multiplier phototube (a FW129 type), on yet another contract.³ In this tube, the limiting aperture and cascade aperture are operated at the same potential and a third and smaller aperture is placed between them to form an einzel lens configuration. The net result of this design is to produce a variable electronic aperture when the center aperture is operated at a negative potential with respect to the photocathode. The ability to adjust the diameter of this aperture thus provides a means of selecting the instantaneous effective cathode diameter (IEPD). As pointed out in an earlier report, restricting the cathode area is a major contributing factor to good counting characteristics.

Figure 16 shows the effect of varying the center aperture from cathode potential (0 volts) to -9 volts. As the potential is made more negative, the IEPD is decreased and a corresponding decrease is seen in the total count. The location of the single electron peak, however, remains unchanged, indicating that the gain of dynode one is not affected. A further interesting characteristic is the nearly constant peak-to-valley ratio. This ratio varies from 1.45 to 1.58 with an average value of 1.51. Of equal importance is the very low dark counting rate. In no case is the total count per channel in the region of the peak more than two, and in other channels one or zero.

It is not yet known if this low dark counting rate is truly a property of this aperture-dynode one configuration since only one such tube has been constructed, but it is of sufficient interest to merit further investigation.

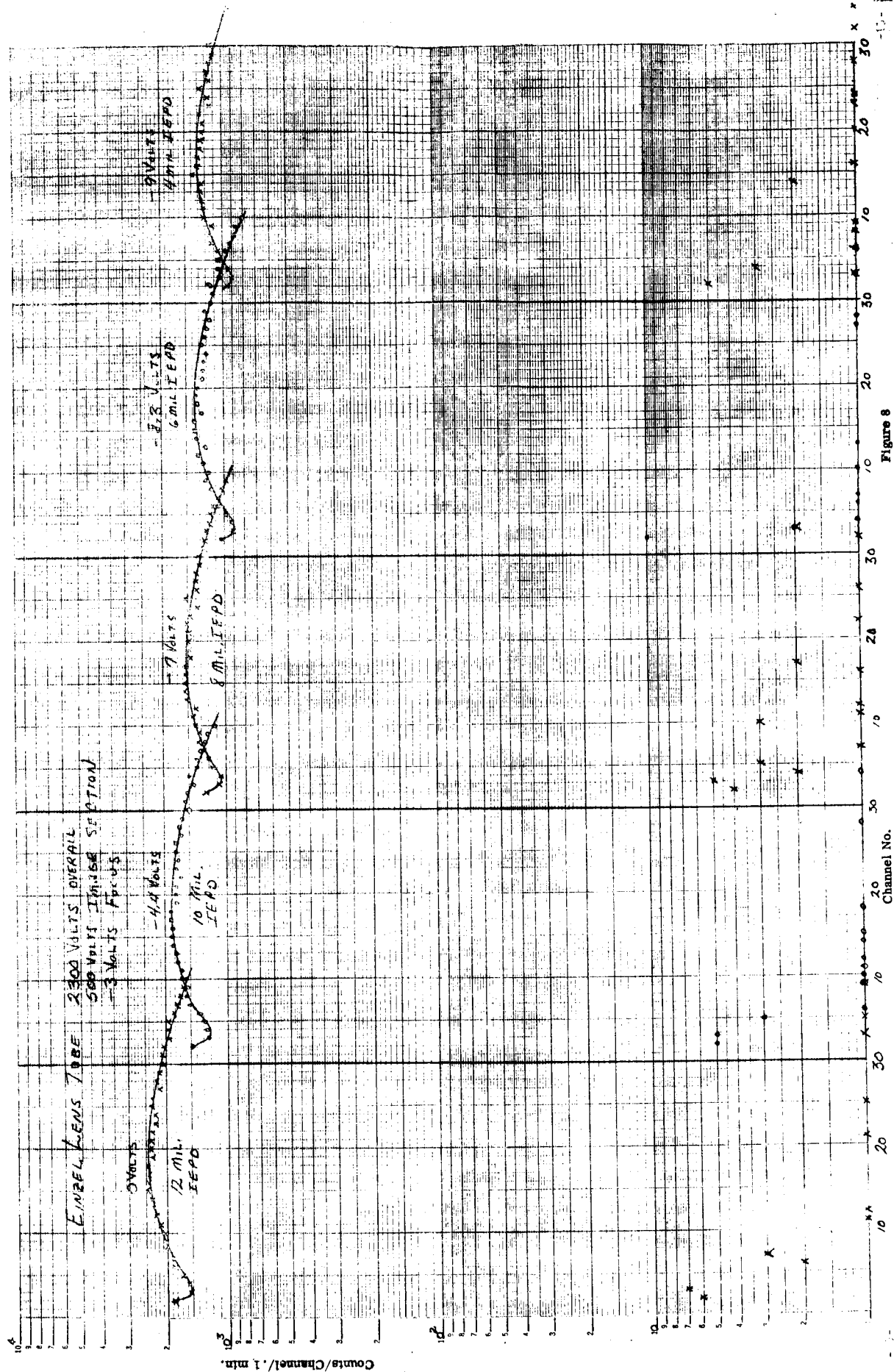


Figure 8

Figure 16

7.0 HIGH QUANTUM EFFICIENCY, MULTI-PASS CATHODES

In the last year or two much interest has been shown in ways to improve the quantum efficiency of multiplier phototubes. In this laboratory, first efforts have been directed toward more efficient use of the incoming radiation at the photocathode.

In the application of a phototube, with a translucent cathode, the radiation enters the cathode at normal incidence. However, a number of events occur which serve to reduce the effectiveness of the input signal.

First of all, some of the input radiation is reflected at the air-glass surface of the faceplate. At the glass-photocathode interface, another reflection occurs while some radiation interacts with the photocathode to produce the desired photoelectrons. Finally, a large fraction of the incident radiation is transmitted into the vacuum space and scattered by reflection off the internal structure of the tube. If the radiation could be made to interact more often with the photocathode, a higher photoelectron yield could be achieved. Figure 17 shows an arrangement which has been tried here with encouraging results. It consists of a prism affixed to the faceplate of the tube. The incoming flux is injected into the faceplate at the critical angle so that it is trapped between the two surfaces and as a result multiple reflections occur causing photoelectrons to be emitted each time the light passes into the cathode layer. Of course, some of the above mentioned losses still occur but it will be shown that the desired effect, namely higher photoelectric yield, due to multiple interaction of the light with the photocathode does, in fact, occur.

A multiplier phototube having an S-20 slit shaped cathode with an effective size of 0.750 inch by 0.080 inch, was built for a NASA user on another contract. The prism was cemented to the faceplate, with Eastman 910 adhesive so that the path of the multiple reflection could be made to coincide with the slit cathode.

Figure 18 shows two spectral response curves for this tube. One is taken with the input radiation flooding the cathode and the other is taken with the input radiation injected through the prism in such a way that the multiple reflections are visible.

In the first case, the luminous sensitivity was measured to be 105 μa per lumen and in the second case it was 230 μa per lumen. The region of peak sensitivity appears to have shifted about 400 \AA but the radiant sensitivity is nearly 0.028 ampere per watt higher for the multiple reflection case. An attempt was made to measure the improvement in the anode sensitivity due to this effect. It was discovered that the angle of incidence of the light on the face of the prism is very critical. It appears that normal incidence of the light on the prism face is not a sufficient condition to assure multiple reflection. For this reason it will be necessary to modify the test equipment to provide the needed freedom and accuracy of adjustment to get this data.

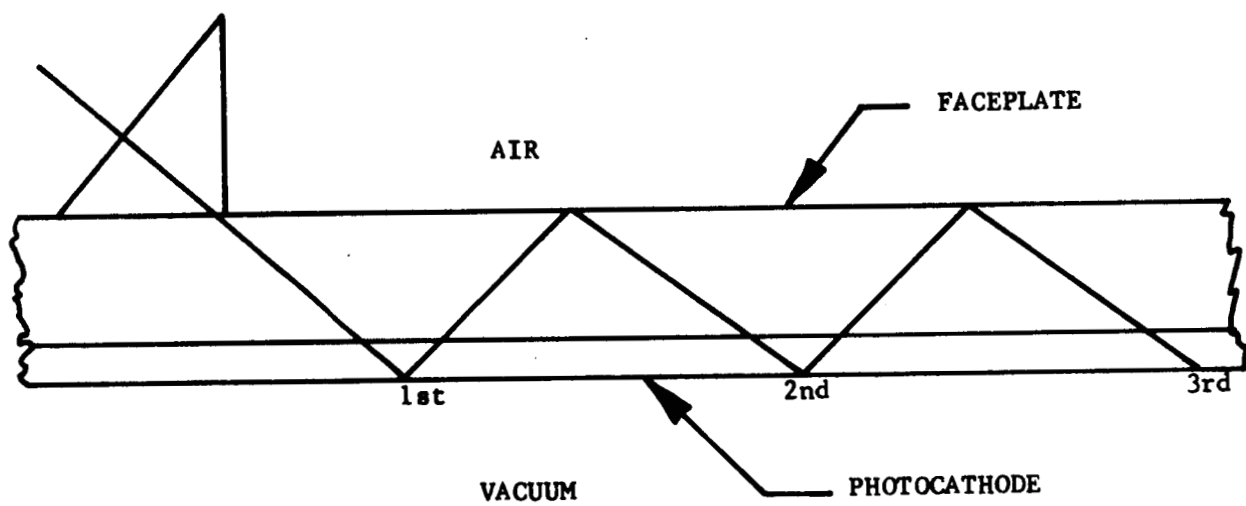


Figure 17

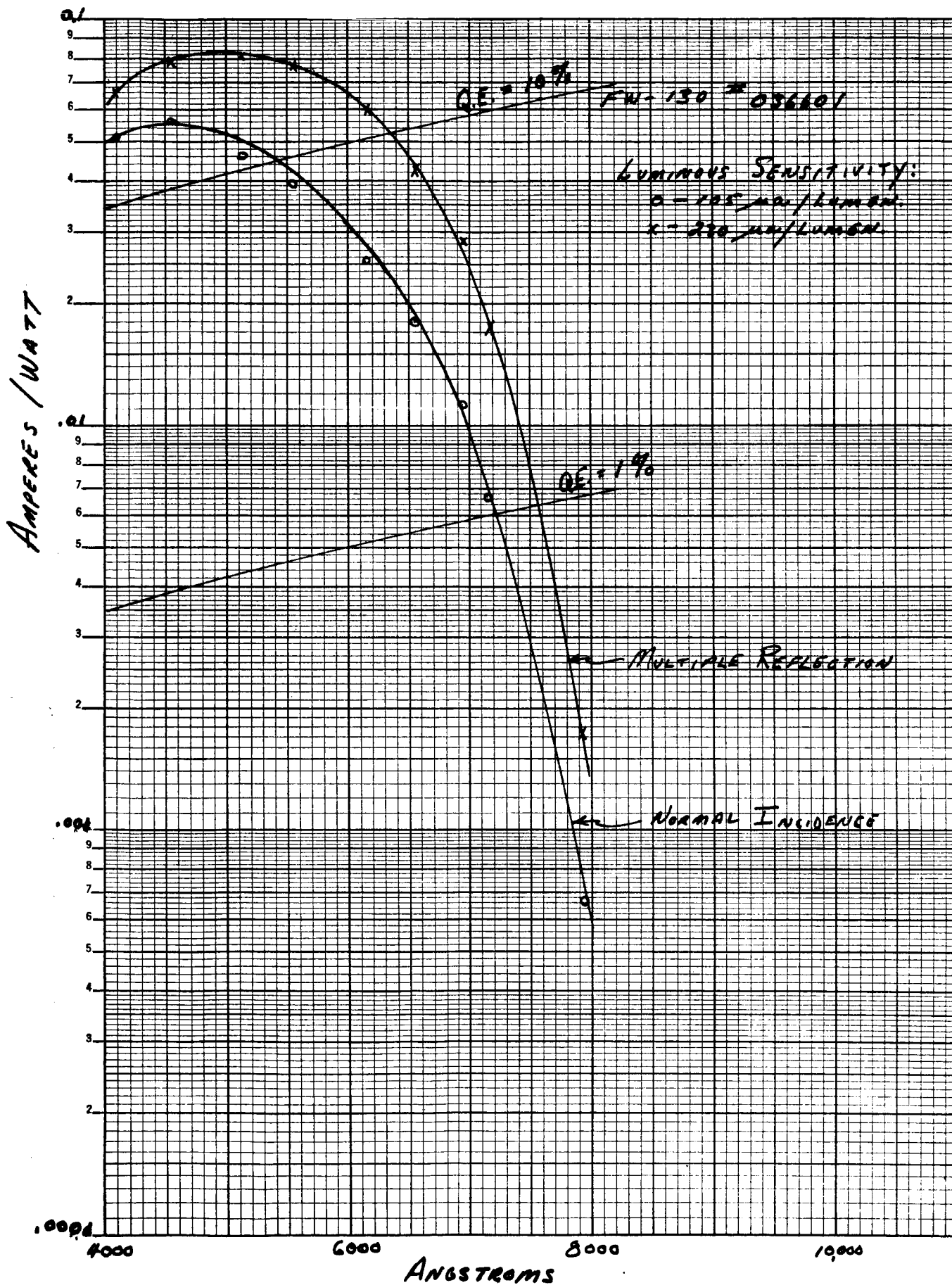


Figure 18

In actuality, the anode sensitivity measurements were nearly identical for the two modes of operation. Figure 19 is the plot of this data for normal incidence on the photocathode.

The single electron spectra of this tube for the two modes of operation is shown in Figure 20. The tube was operated at 1800 volts with dynode one at -30 volts with respect to the aperture electrode, and the light was injected into the prism with a flexible fiber optic light guide. In this tube, -30 volts on dynode one produced the same results, as far as the pulse height distribution is concerned; as does a negative potential on the cascade aperture in tubes reported previously. This may be due, in part, to the fact that the slit aperture confines the primary electrons to a long narrow area at the center of the dynode where dynode-one bypassing is less likely. A more probable explanation of the observed improvement is the fact that the secondary electron collection efficiency is more uniform for an aperture of this shape. It is obvious, from the two upper curves, that the injection of the signal through the prism does not in any way destroy the tubes ability to detect single events at the cathode. The peak-to-valley ratio for these two conditions of operation remains at 1.65. The slight difference in the peak height is due to the inability to exactly duplicate the light level. Here again, as in the case of the responsivity measurements, there is difficulty in assuring that multiple reflections do in fact occur since the level of illumination is so low as to be imperceptible, and more accurate methods will have to be devised to adjust the angle of incidence at higher light levels in order to visually optimize the reflections.

The dark count is almost entirely cathode originated as can be seen by the shape of the distribution curves. If the cathode is biased off to dynode two potential, there is further evidence of the origin of the dark noise for now the dark count is down to less than two counts per second. As well as being few in number, these counts are located in the early channels of the spectrum where they would not add appreciable error to the detection of pulses of the most probable amplitude.

MODEL

DATE

DARK CURRENT (AMPERES)

 10^{-1} 10^{-2} 10^{-3} 10^{-4} 10^{-5}

1.4

1.6

1.8

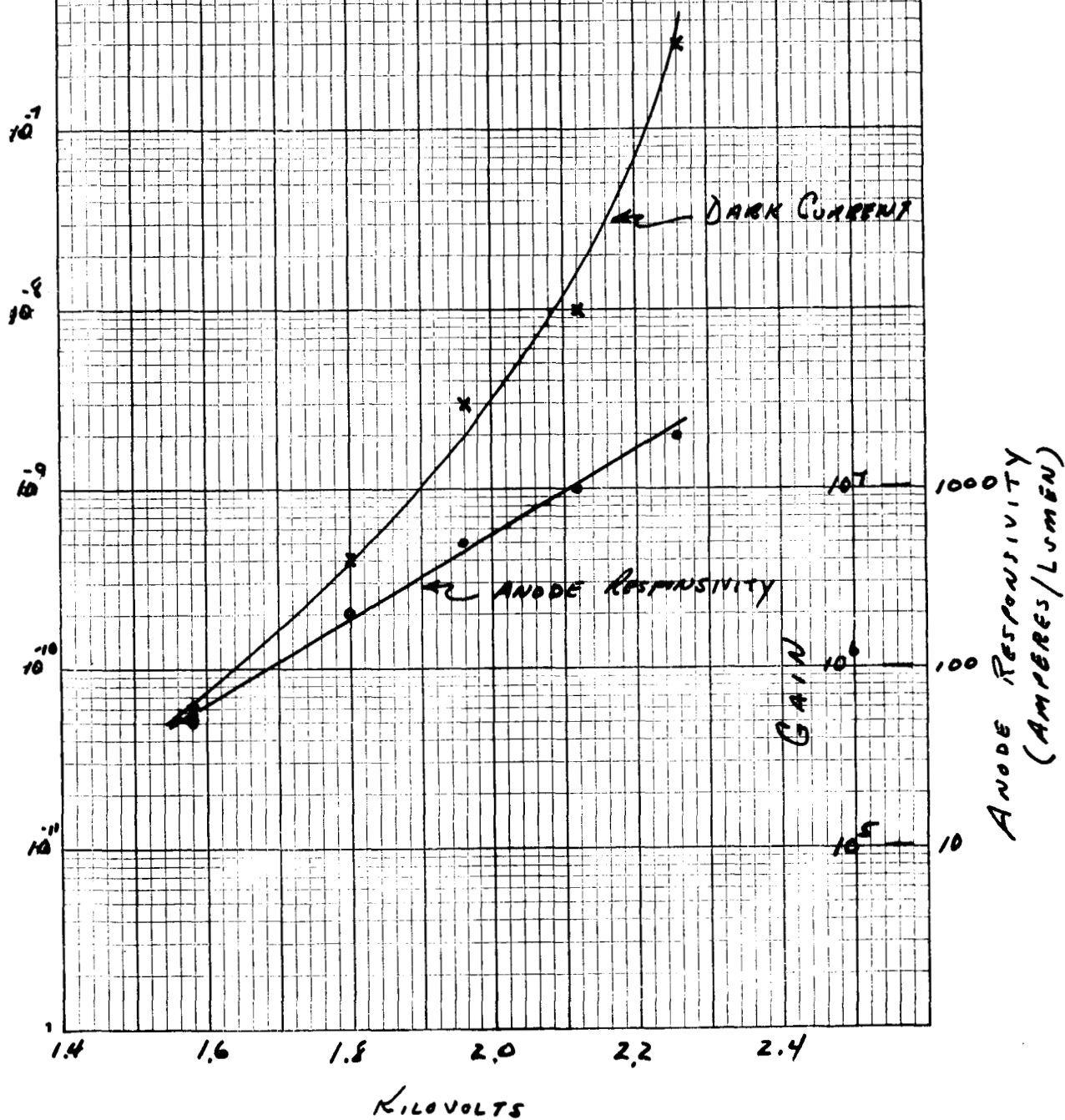
2.0

2.2

2.4

KILOVOLTS

Figure 19



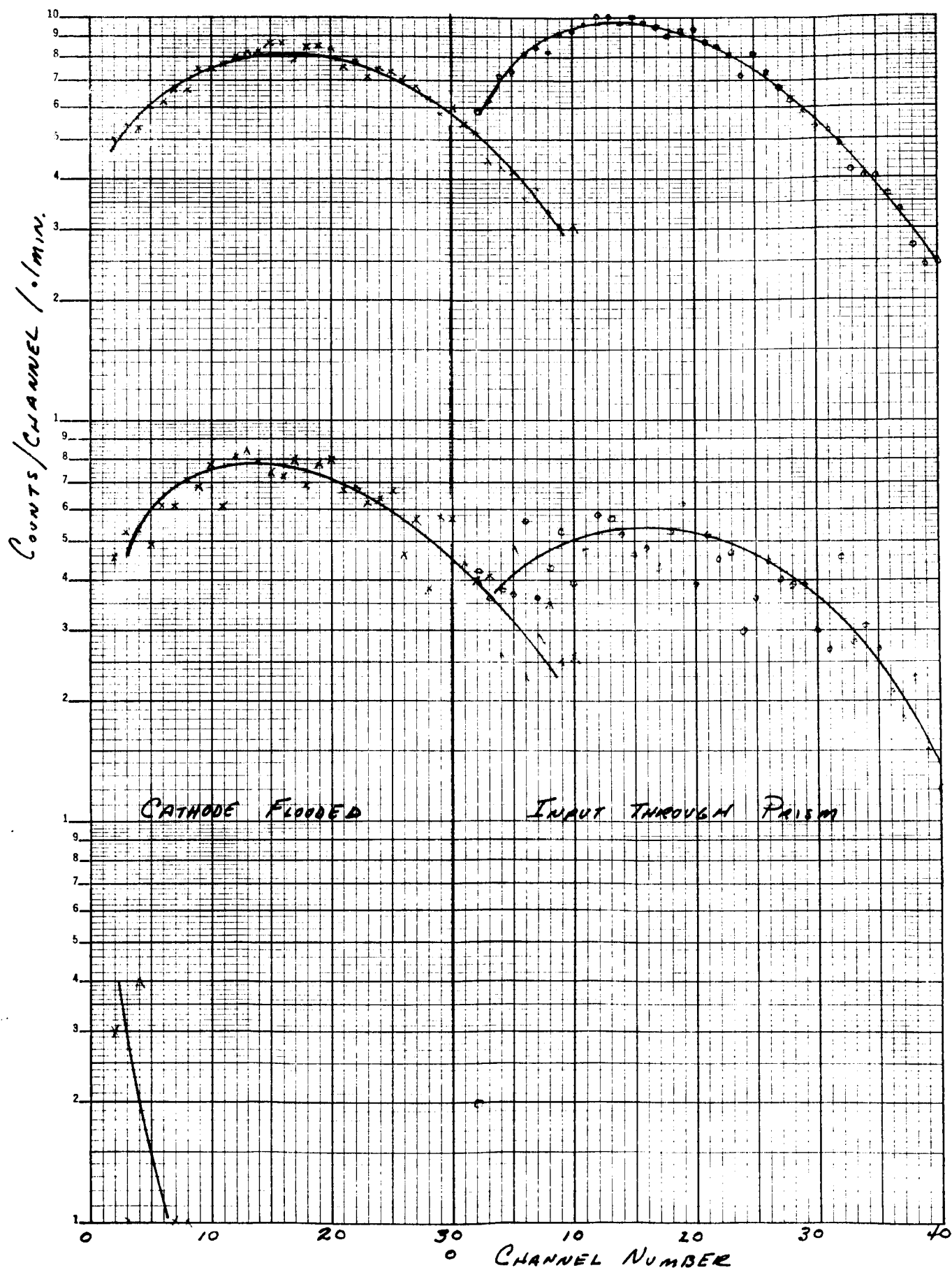


Figure 20

8.0 LARGE EFFECTIVE PHOTOCATHODE AREA

The diameter of the effective photocathode of the majority of ITTIL multiplier phototubes is of the order of 0.100 inch, though somewhat larger cathodes may be obtained by proper selection of the aperture diameter. The maximum effective cathode diameter is, of course, set by the diameter of the actual formed photocathode (0.750 inch), though the practical limit may be somewhat less than this. This limit, however, may not be obtained simply by changing the physical aperture diameter because of dynode size limits. In addition, the magnification of the electron optics as well as the area of dynode one must be changed in order to accommodate the larger photocathode diameters.

Presently, a tube having an 0.5 inch effective diameter cathode and a 12-stage multiplier is under development for a NASA customer⁵ and test data on a sampling of these tubes is presented in this report. Figure 22 is a photograph of a typical tube of this type. The image section of these tubes is of the same design as the standard FW Series of multiplier phototubes except for modifications required to produce a magnification of 0.4 instead of the usual value of 0.7, for the reasons mentioned above. The photocathode may be any one of several types formed on the vacuum side of the entrance window which is sealed into the metal cathode sleeve. Connections to the cathode are made by way of this sleeve.

Two methods of cathode processing have been used. In both cases, the channels for evolution of the alkali metals were placed in an external bulb attached to the tube by the tubulation nearest the cathode. In most of these tubes, the antimony evaporator was permanently mounted in the tube, while in one the antimony evaporator was inserted on a retractable member, through the same tubulation so that it could be removed after the evaporation process. This type of evaporation has not produced a satisfactory high sensitivity cathode as yet; however, the tube was operable. This method leaves the tube completely free of processing leads, thus simplifying the internal tube structure.

The multiplier section, as can be seen in Figure 21, is enclosed within a metal sleeve separating the image section and the glass stem, hopefully reducing dark noise. This metal sleeve is also the defining aperture terminal. The cascade aperture and all dynode leads are brought out through a 13 pin stem while the coaxial lead at the center of the stem serves as the anode connection. While this connection is a standard subminiature 50 ohm connector, no attempt as yet has been made to maintain this ultra-low impedance, configuration inside the tube. The load impedance used in most of the tests is of the order of 10^5 or 10^6 ohms.

Performance characteristics of this tube include the ability to count single events at the cathode as well as improved rise and transit times, compared to the standard line of ITTIL multiplier phototubes.

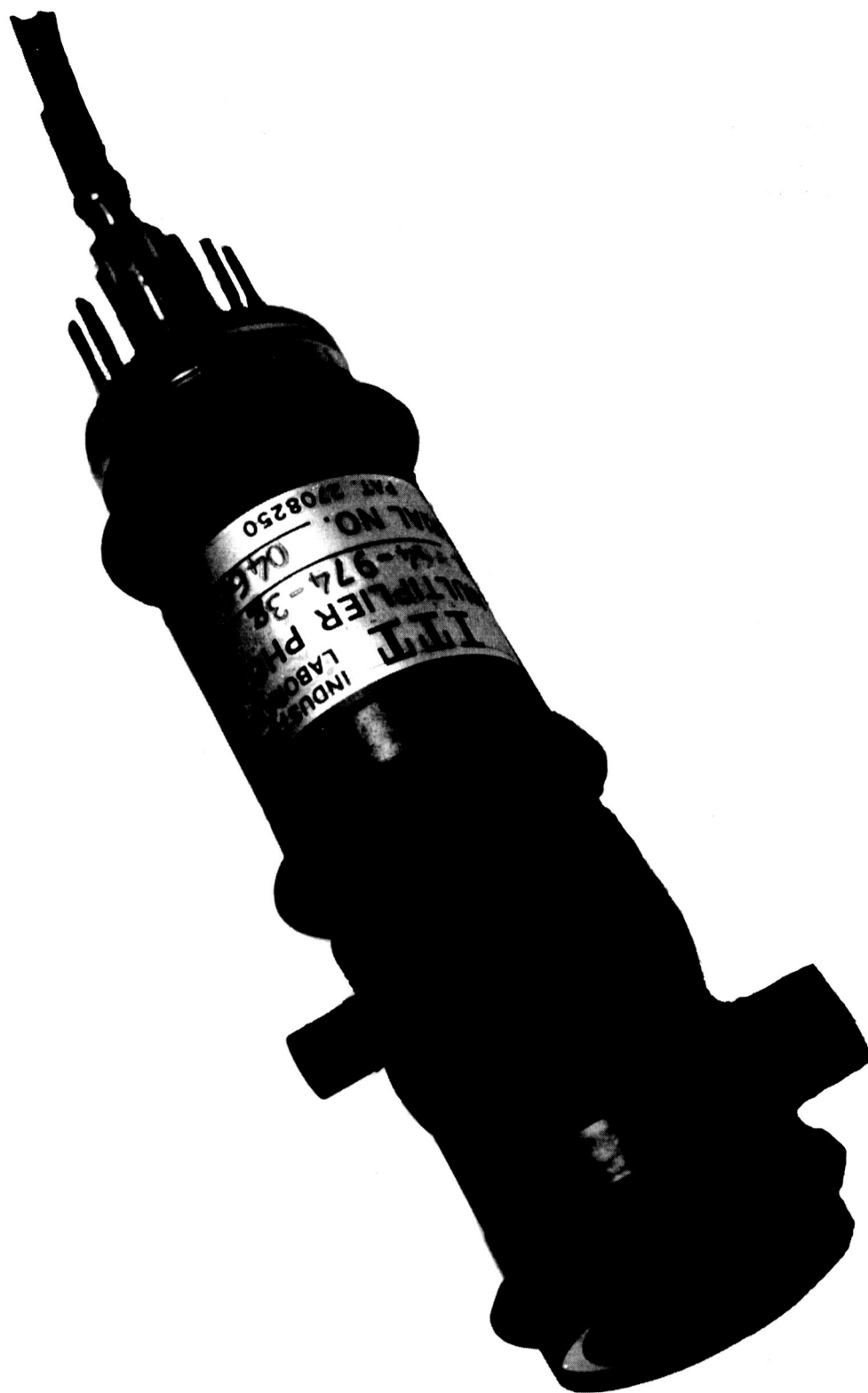


Figure 21

8.1 Cathode Characteristics

The four tubes which are reported on here have S-20 type cathodes on a sapphire window. Tubes of this same design but with S-11 cathodes are also being built but prototypes were not available for final test at this writing. The spectral response of these four cathodes is shown by the solid line in the plot of Figure 22 while the dashed curve is the typical response of an S-20 surface formed on a visible light transmitting window,⁶ such as 7056 glass which is normally used in this laboratory. The short wavelength limit of the solid curve is set by our present means of measuring this parameter, namely a calibrated tungsten 2870 degrees K lamp and a set of Optics Technology narrow bandpass filters. At present, a McPherson model 235 Vacuum UV Monochrometer is being readied for operation which will permit measurements of this type to be made down to 1000 Å. It is safe to predict, however, that the response of these cathodes should have the same general shape below 4000 Å as the S-13 surface (Cs-Sb on fused silica) which has extended ultraviolet response due to the transmission of the window material.

In order to determine the effective photocathode size and the response uniformity, the photocathode was mechanically scanned with a small spot of light while the output of the multiplier was monitored with a d-c oscilloscope. Figures 23 and 24 show the plots of this data as a function of displacement along two mutually orthogonal diameters, one of which is parallel to dynode one.

The curves marked (a) are plots from left to right along the length of dynode one and those marked (b) are plots from the open side, towards dynode two, to the back of dynode one. It should be remembered that, the electron lens produces an inverted image so that nonuniformities on the one side of the cathode are superimposed on nonuniformities on the opposite but corresponding side of dynode one. The gross nonuniformities of the output signal are for this reason, a composite of opposite halves of cathode and dynode one. It has been shown, however, in an earlier report on this project⁷ that the cathode shading in general is not nearly pronounced enough to account for the total output signal shading but that the gain of dynodes one and the collection efficiency for dynode two account for the largest portion of this effect. This data shows clearly, however, that the effective cathode dimensions are about 0.6 by 0.5 inch when measured at the half amplitude points of these curves. The downward deflection of the scope trace, for maximum signal, is due to the negative going voltage produced across the load resistor by the output current.

8.2 Multiplier Response Time Characteristics

Aside from the usual electron multiplier characteristics, such as gain, dark current, ENI, etc., the single pulse transit time is of particular interest since this tube is to be used to detect signals which range from those able to excite only single electrons from the photocathode to those of such intensity as would produce a dc anode output due to pulse overlap.

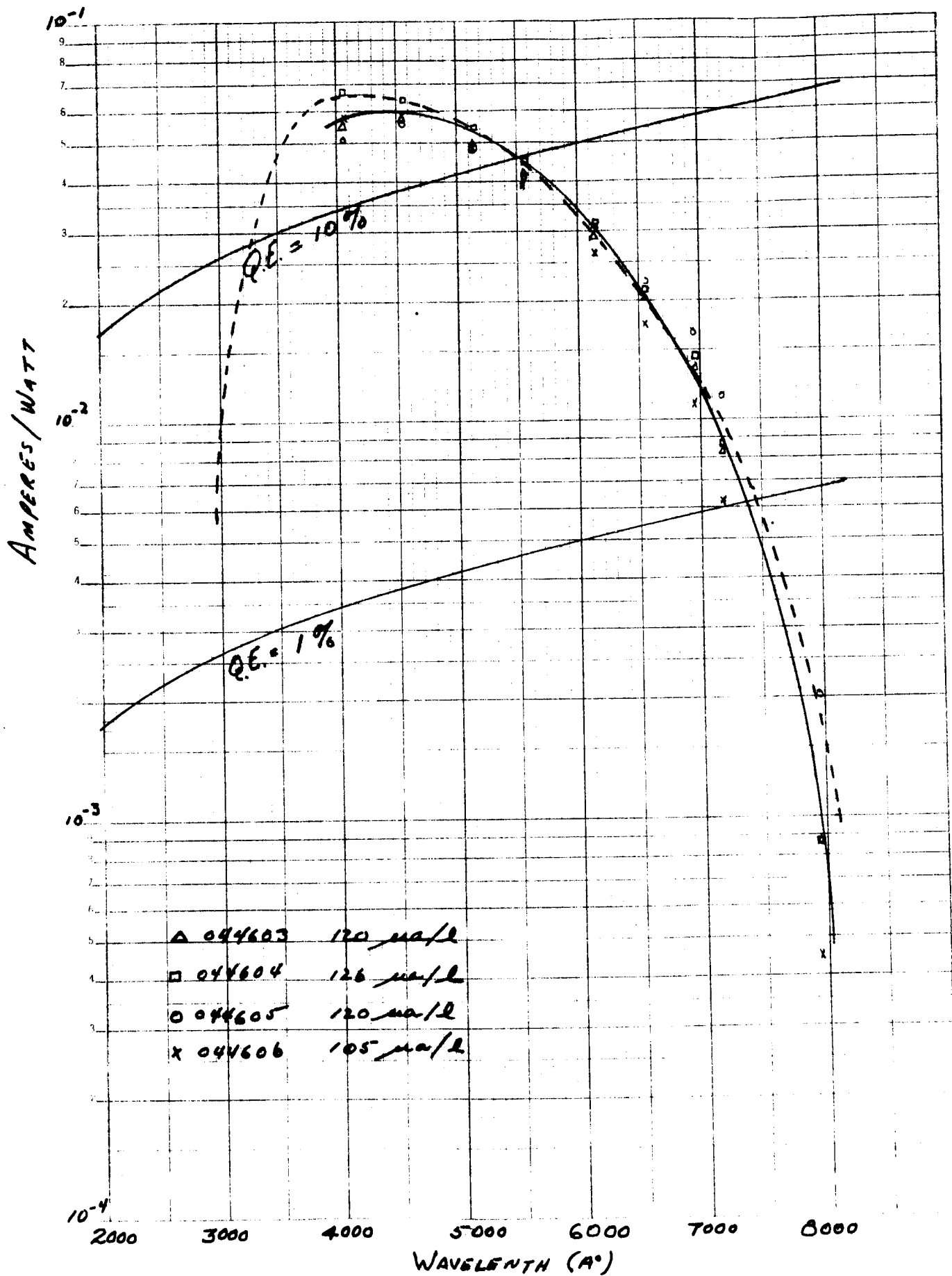
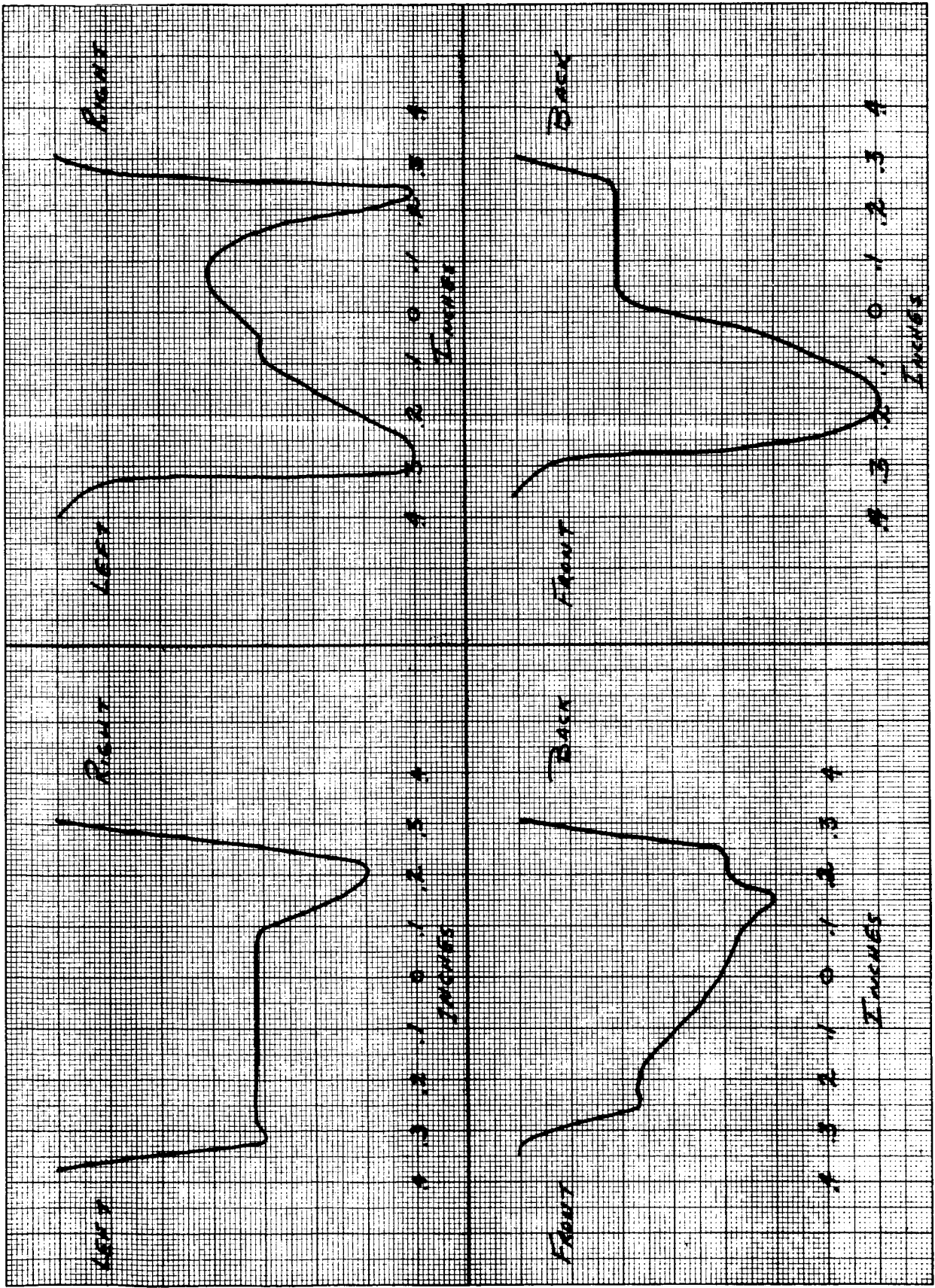


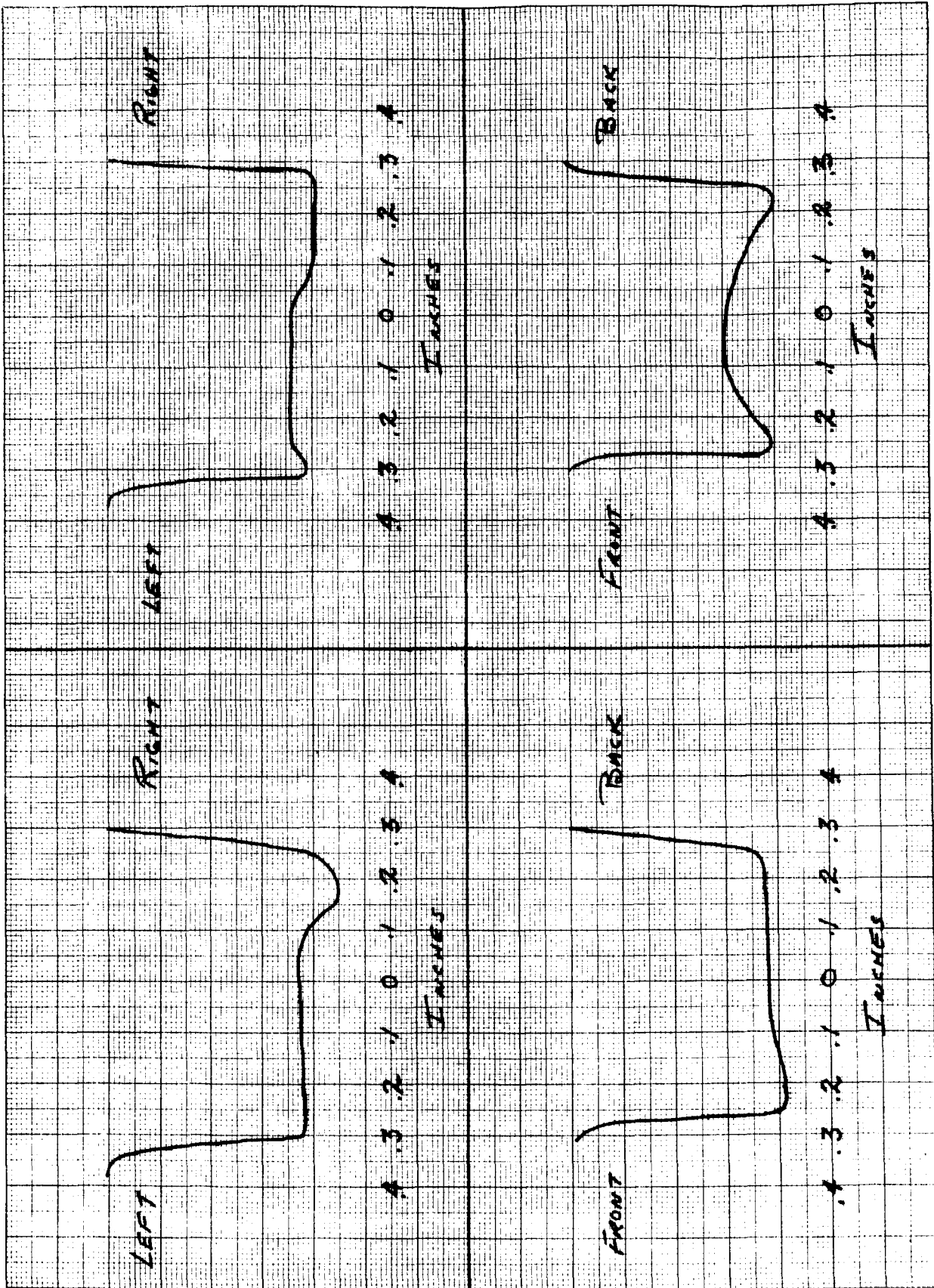
Figure 22



046604

Figure 23

046603



046606

Figure 24

046605

Figure 25 is a block diagram of the special test equipment used by ITTIL to make the required response time measurements. It consists essentially of a high speed triggered light source which illuminates the multiplier under test, and a photodiode. The output signals from these tubes are fed to a dual trace sampling scope whose time base is also triggered by the light source. Since this process is controlled by a trigger generator at a regular occurring rate, the oscilloscope presentation shows these events in their proper time relationship.

Figure 26 shows these oscilloscope presentations for the specified operating conditions. In Figure 26a, the tube is operated as indicated with the cascade aperture (A_2) connected to dynode one and the defining aperture. The larger negative going trace is the multiplier output and the photodiode output is the sharp spike at the left side of the photograph.

The time separation between these two signals is the transit time of the multiplier tube and is approximately 40 nanoseconds with a rise time of 10 nanoseconds, a fall time of 30 nanoseconds and a full width at half the maximum amplitude (FWHM) of about 28 nanoseconds. Figure 26b shows virtually the same results with the cascade aperture (A_2) at -45 volts with respect to dynode one and defining aperture. However, in Figure 26c, when the cascade aperture is again at dynode one defining aperture potential but with increased image section voltage and constant multiplier voltage (to maintain constant gain), the transit time is 30 nanoseconds. In all cases, the rise time (10 to 90 percent) is 10 nanoseconds. The voltage distribution in (c) is typical of the conditions under which the tube is pulse counted though the over-all voltage is somewhat higher than required. The test light pulses are so short (approximately 1 nanosecond, FWHM) that the output current pulses from the tube are essentially identical to those generated by single electron events, but with much larger, more easily observable magnitudes.

In the foregoing test, the rather high operating voltage is required in order to develop the necessary output voltage across the 50 ohm load impedance.

With the above information and a knowledge of other conditions such as multiplier gain, pulse processing methods and tolerable number of lost pulses, a calculation can be made as to the maximum permissible dc output current which will keep the pulse rate just below the time resolution limit of the phototube.

8.3 Pulse Amplitude Distribution Characteristics

Figures 27 through 30 are the single electron spectra of these tubes with their respective dark noise spectra. In all cases the cascade aperture was operated at a potential of -30 to -45 volts with respect to dynode one and the defining aperture. In Figure 27, tube number 046603 shows a markedly lower dark count than the other three, though the dark spectrum does show the same general shape as the signal spectrum. The other three tubes have much higher dark count and the distribution is just like that of the signal spectrum.

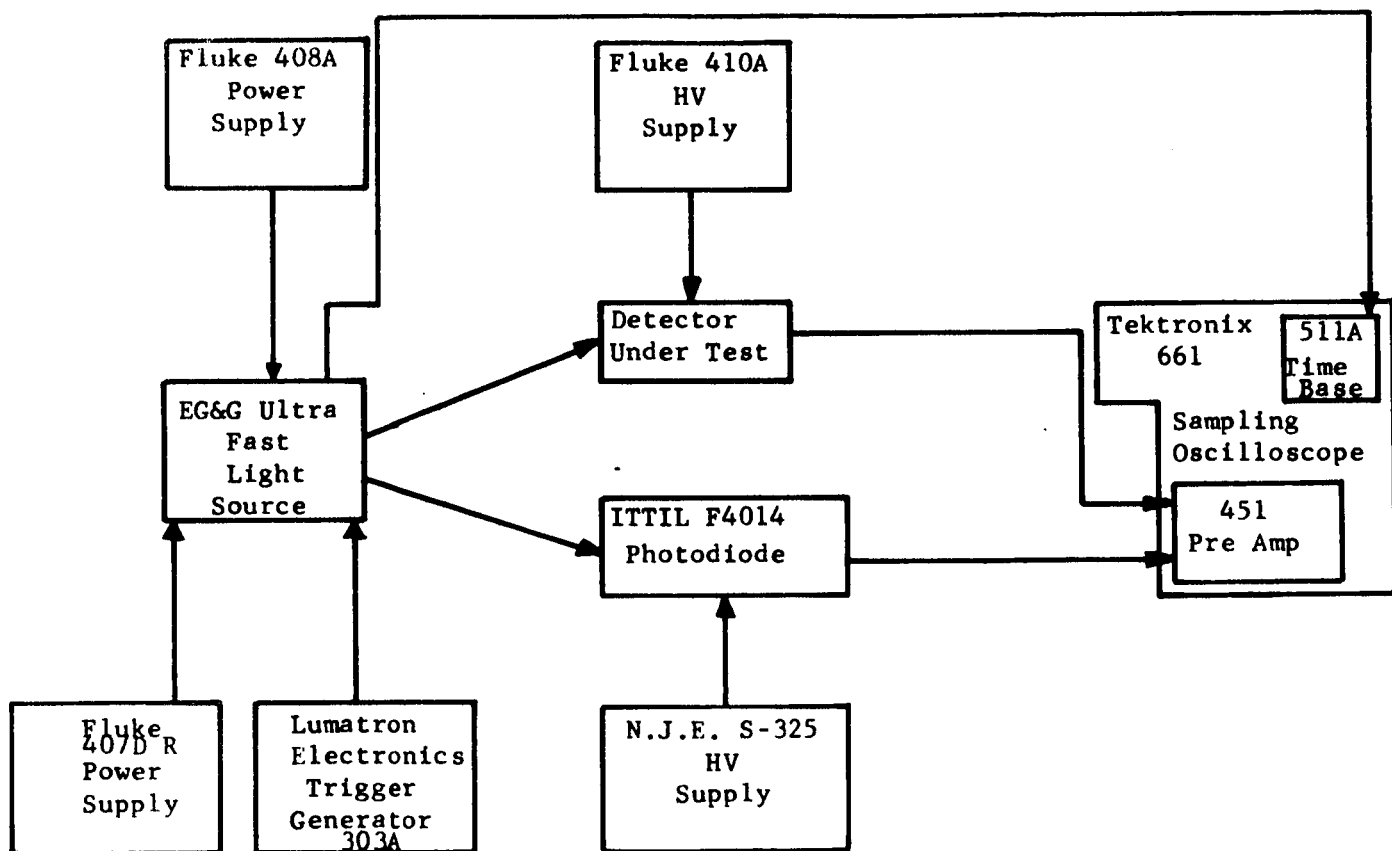
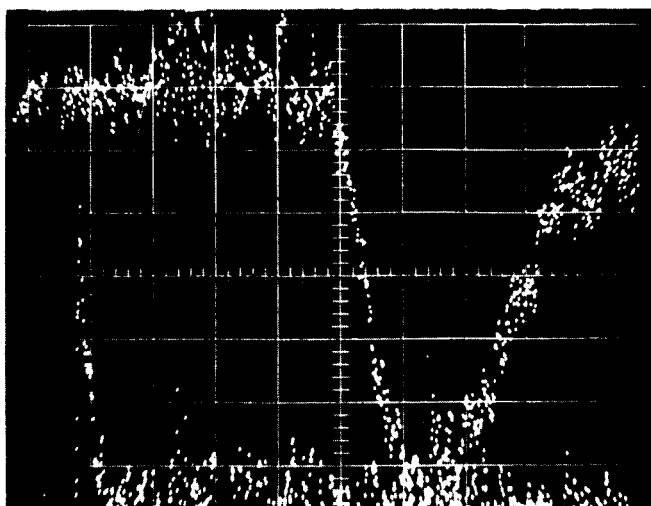
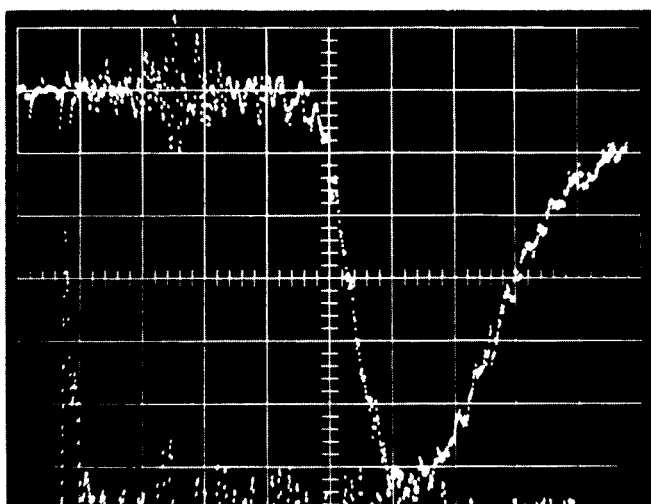


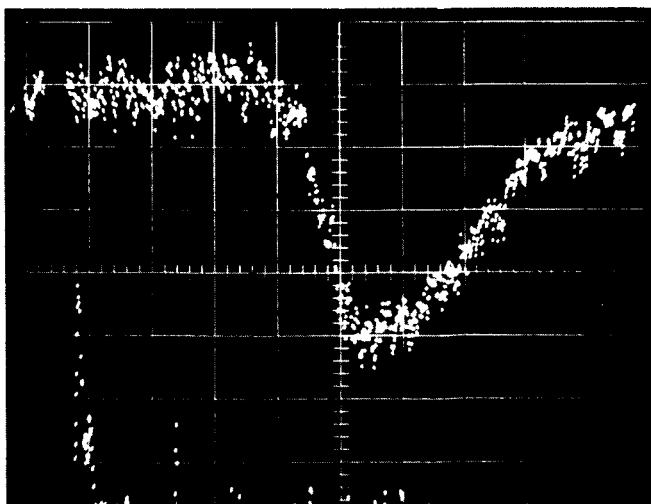
Figure 25



(a) 2000 Volts, 285 Volts Cath- D_1
 A_2 at $A_1 D_1$ potential
 $V = 1 \text{ ma/cm}$
 $H = 10 \text{ nsec/cm}$



(b) 2000 Volts, 285 Volts Cath to D_1
 $A_2 -45V$ with respect to $A_1 D_1$
 $V = 1 \text{ ma/cm}$
 $H = 10 \text{ nsec/cm}$



(c) 2600 Volts; 830 Volts Cath to D_1
 A_2 at $A_1 D_1$ potential
 $V = 2 \text{ ma/cm}$
 $H = 10 \text{ nsec/cm}$

Figure 26

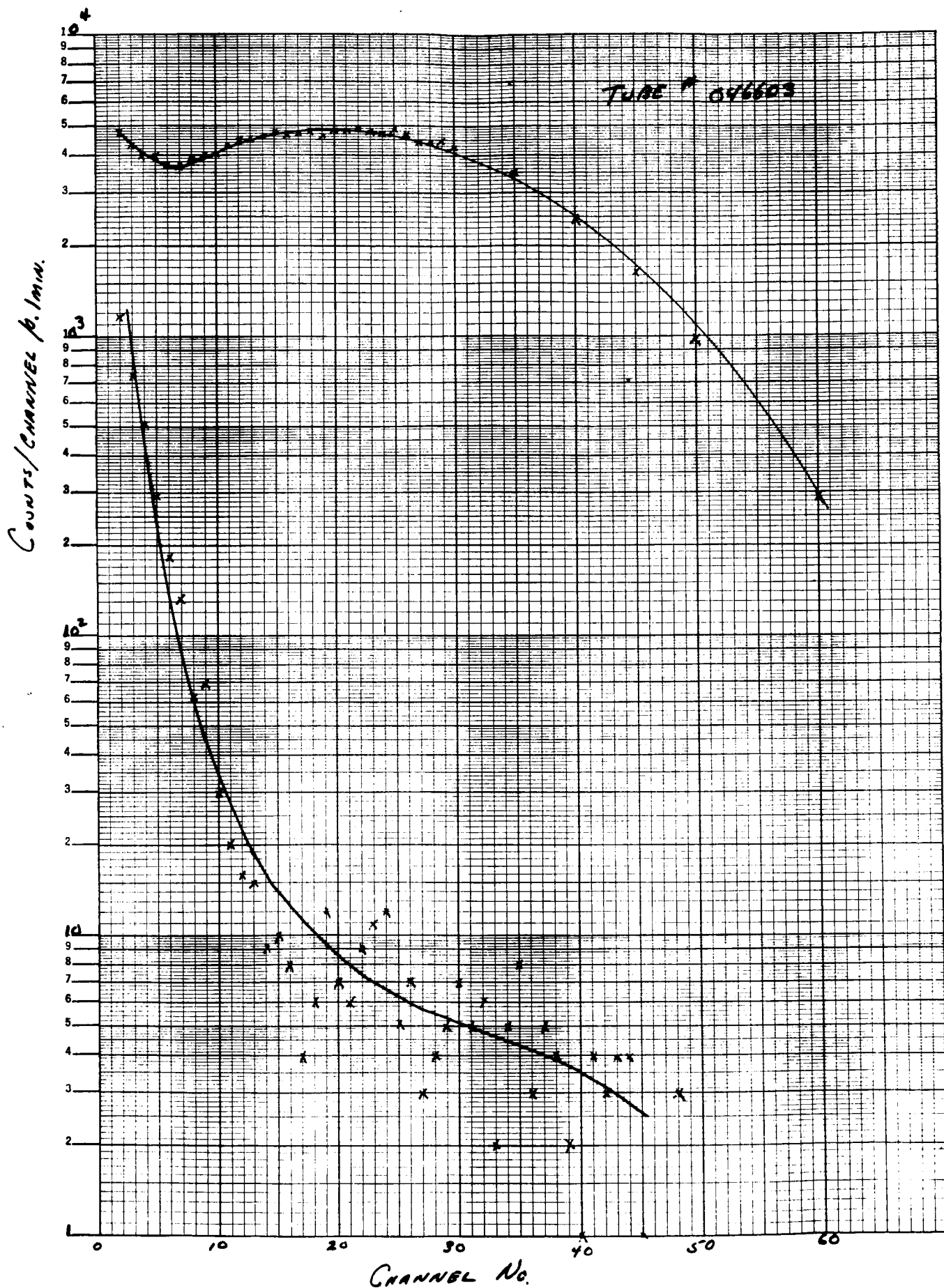


Figure 27

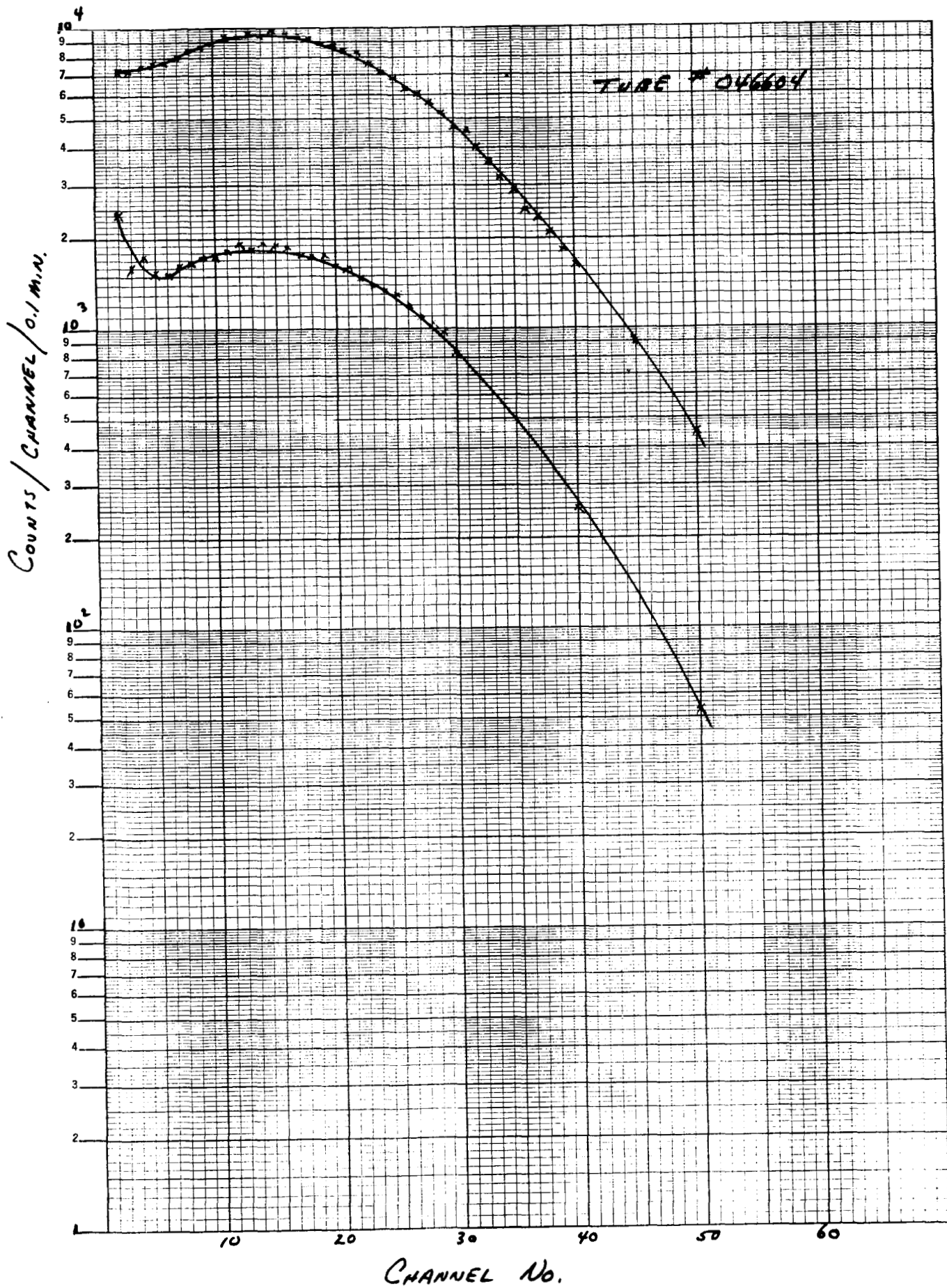


Figure 28

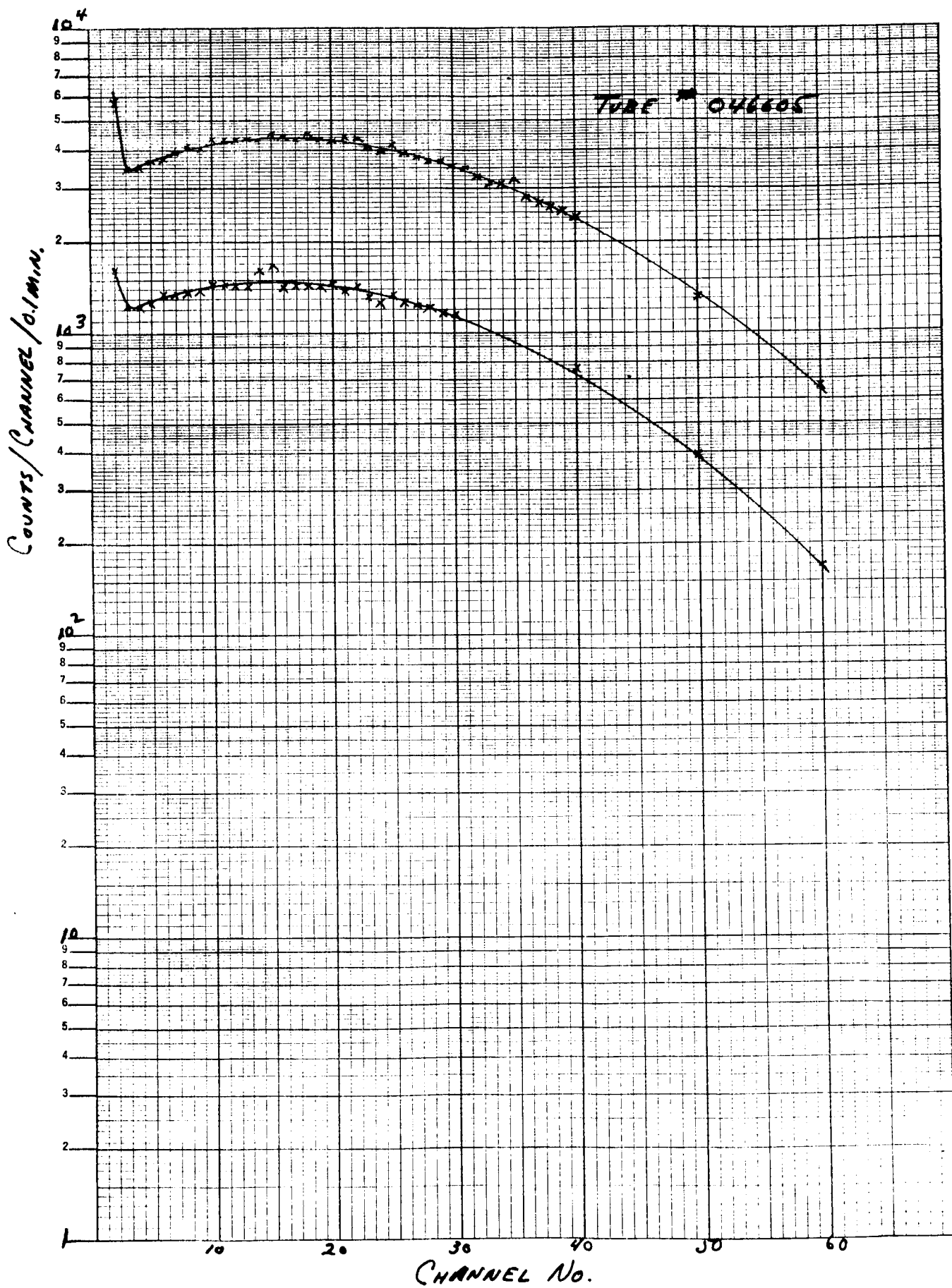


Figure 29

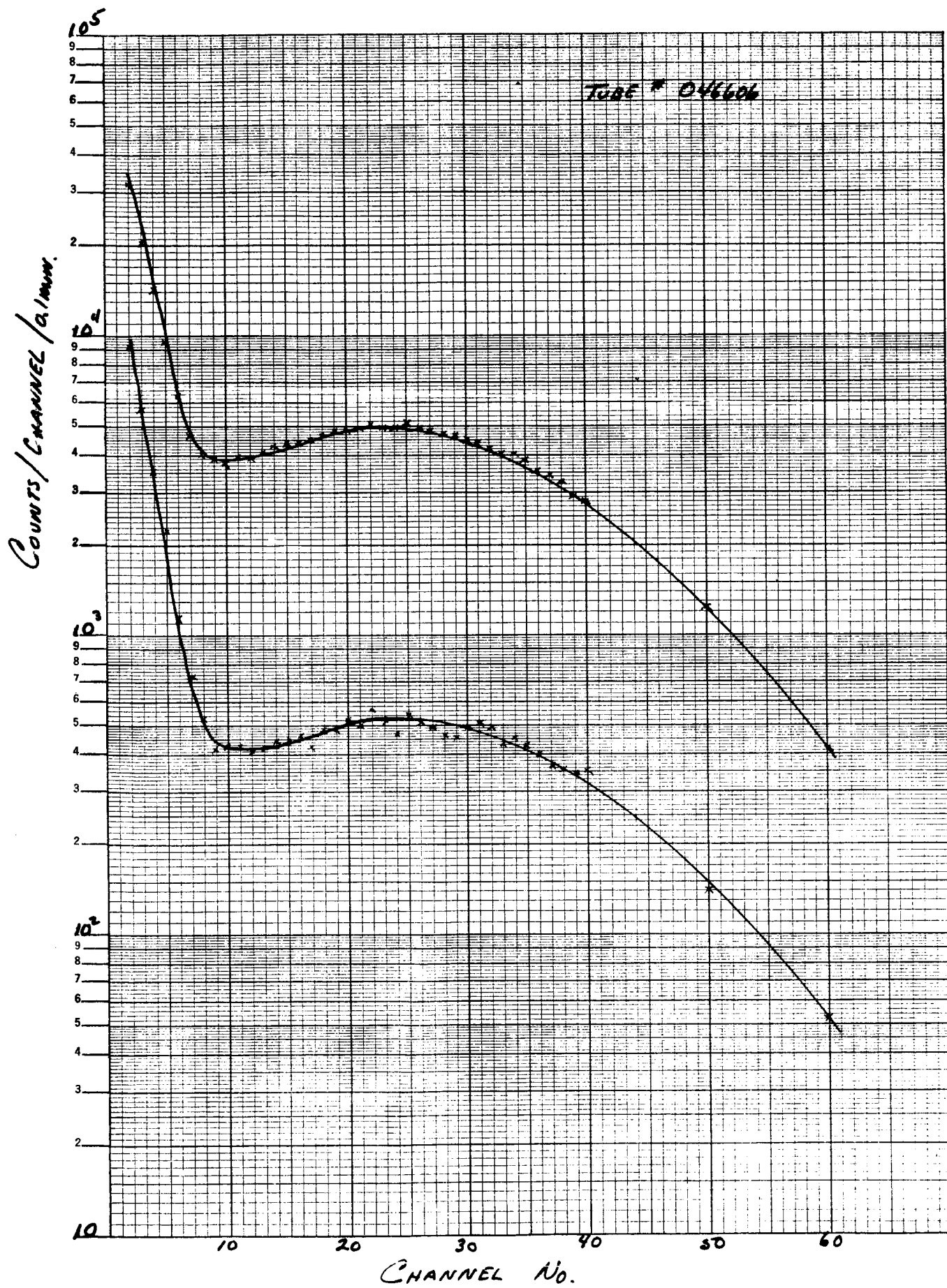


Figure 30

If, however, the cathode is biased off to dynode two potential, these dark pulses are almost entirely eliminated and are not shown on the plots.

This fact is taken to indicate that these tubes would cool well, and in fact, a communication from the customer at this writing reports a dark counting rate of a few counts per second, in dry ice temperatures, for one tube.

A recurring problem in these tubes has been the presence of large pulses not associated with the signal input to the photocathode. A preliminary test of a tube like the ones just described (but with an S-11 type cathode) showed poor statistics with the cathode excited in the usual manner and the single electron peak could only be resolved when the dark count was subtracted. An inspection of the scope monitoring the input pulses to the analyzer showed that many large pulses were also present. It was also observed that the number of these pulses varied with the image section voltage. In order to investigate this effect the analyzer was adjusted so that it counted pulses whose amplitude fell within the region from channel 50 to 150. Since the single section peak was centered about channel 15, pulses falling in channels 50 to 150 represent pulses of from 5 to 10 electrons. Figure 31 shows the total number of pulses in this region plotted against the voltage applied across the image section. During these tests the voltage across the multiplier was held constant in order that the over-all gain of the system did not change. This seems to be a clear indication that the source of these larger pulses is in the image section.

Two other parameters of interest for these tubes are shown in Figures 32 and 33, namely anode responsivity and dark current.

Inspection of these two curves shows that at a gain of 10^6 the dark current ranges from 1 to 2.5 nanoamperes. Tube number 046603 had very unusual dark noise characteristics which certainly must contribute to that fact that it has the highest dark current of the four. Figure 34 is a series of three photographs of the output of the pulse preamplifier due to this noise. Careful examination of this tube during operation at 2500 volts, located electrical discharge visible to the dark adapted eye, in the region of the stem leads. However, the cathode was biased to dynode two so that the possibility of optical feedback to the cathode is ruled out. At lower voltages the noise persisted but was not visible. These results indicate that the noise was coupled to the tube output by direct stem leakage.

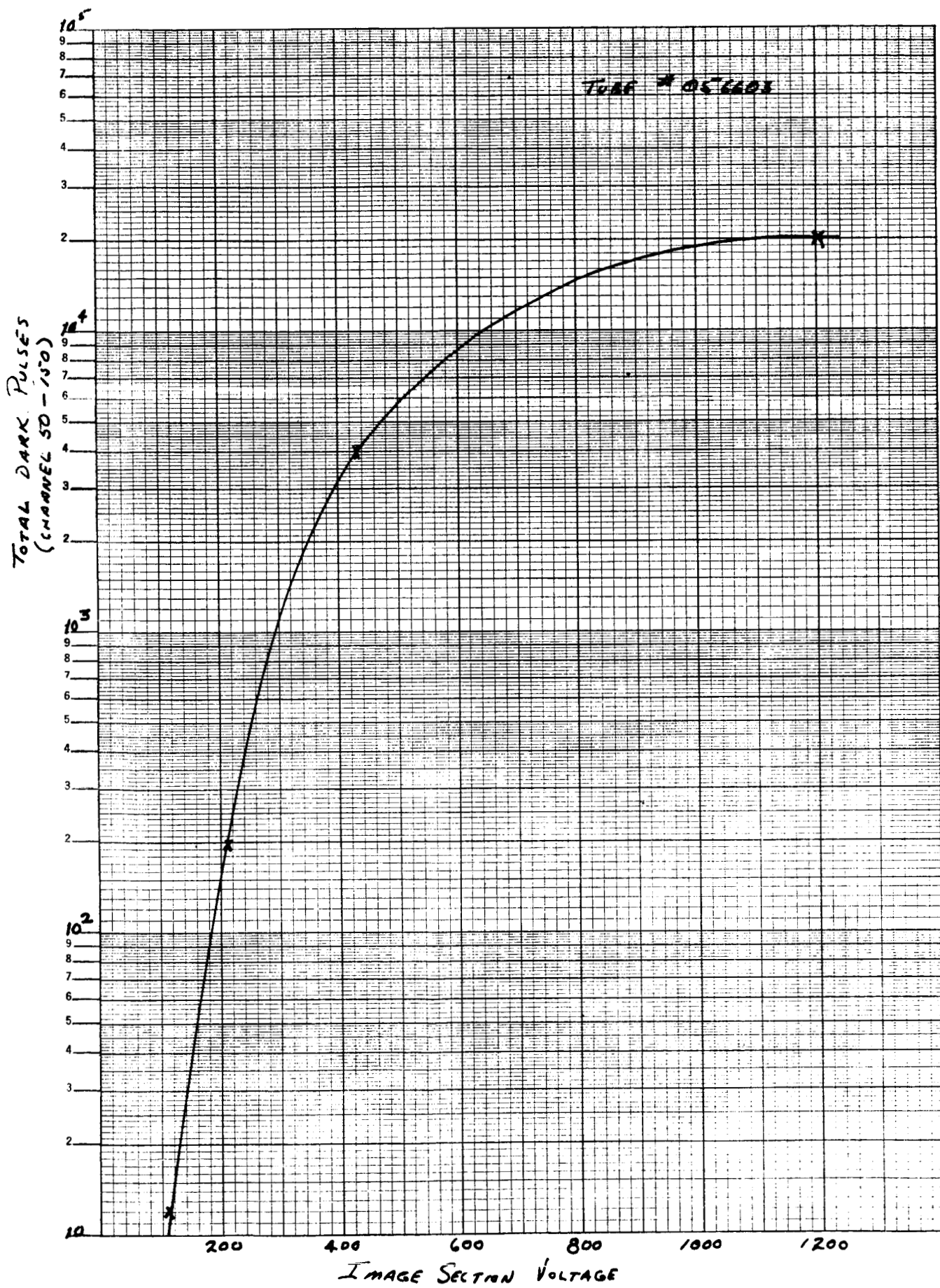


Figure 31

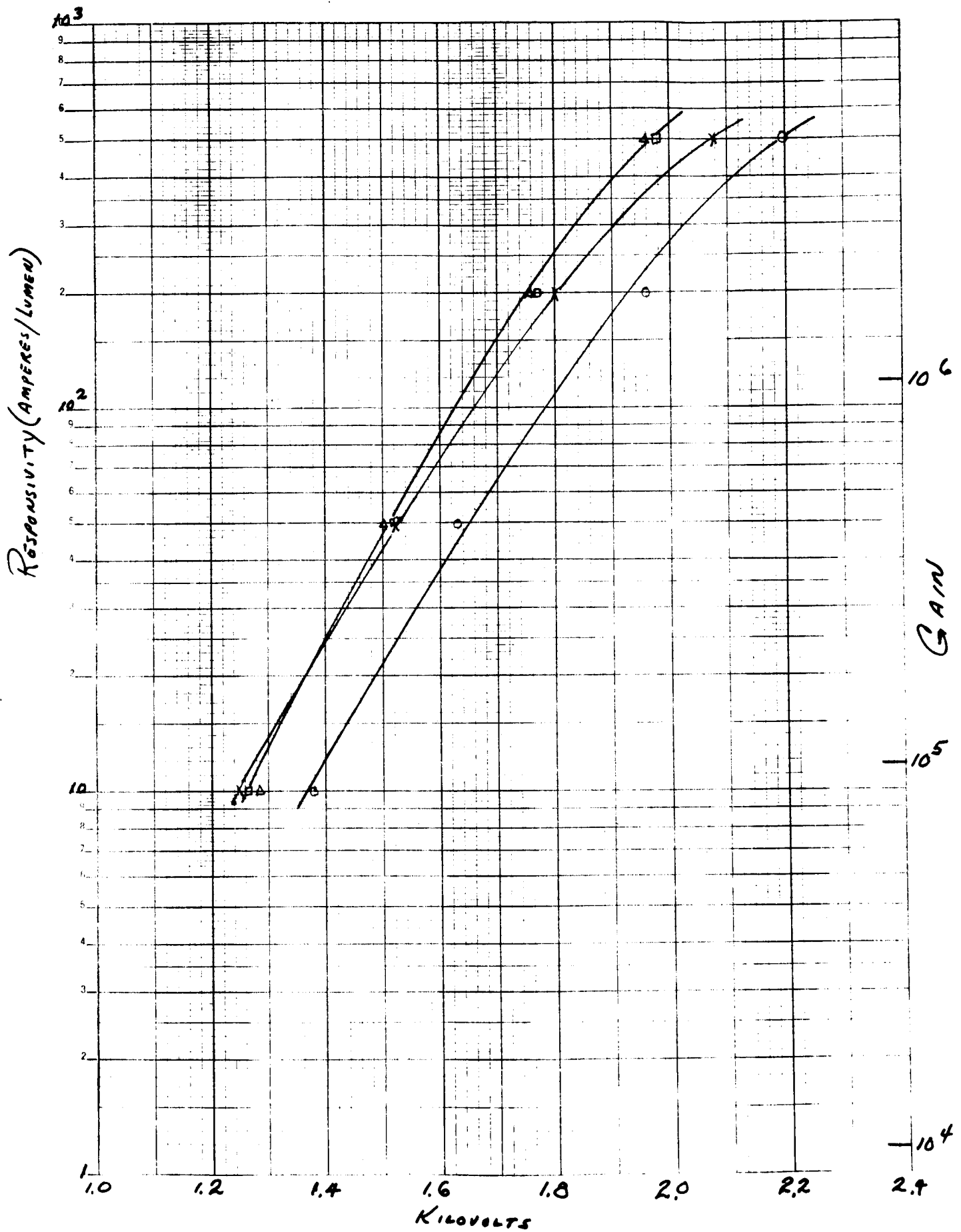


Figure 32

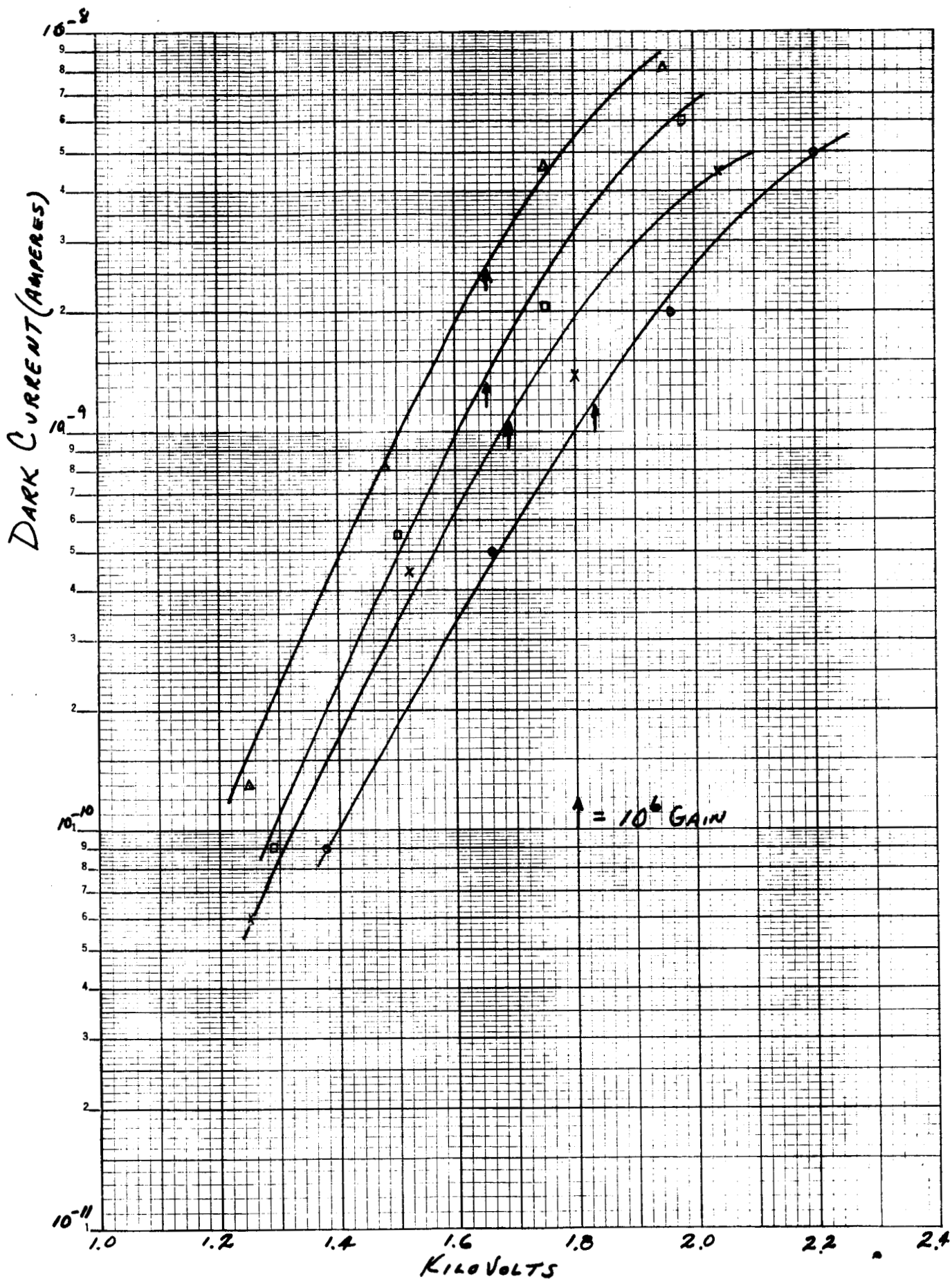
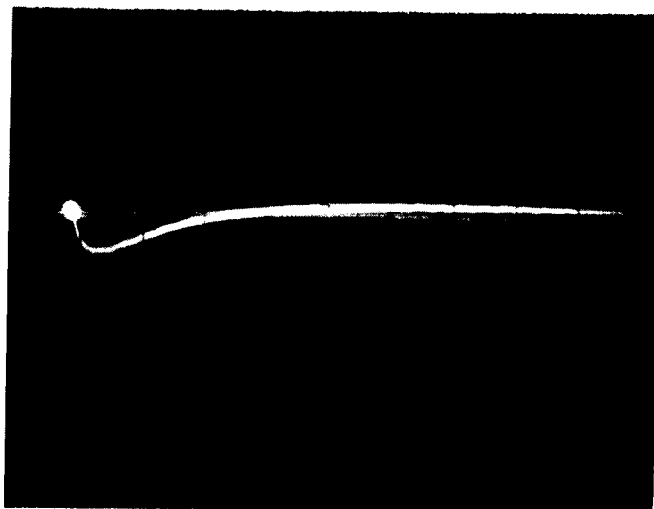
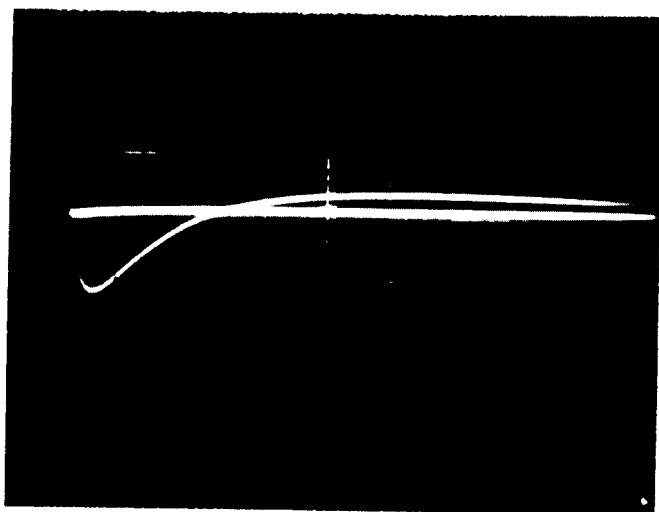


Figure 33



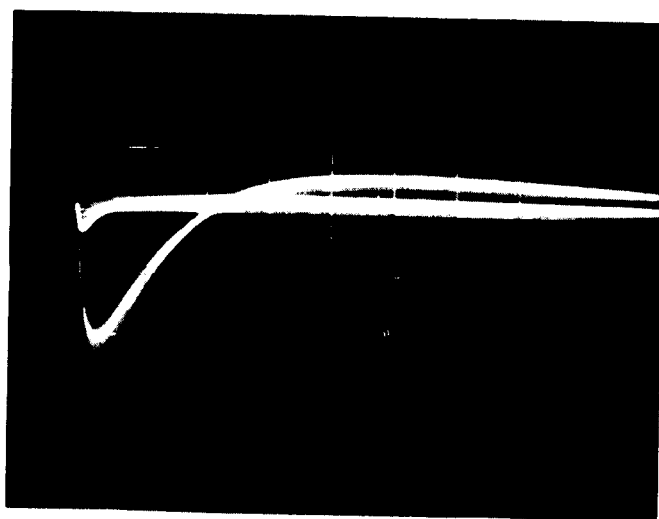
1800 Volts, cathode at D_2 potential

$V = 1\text{v/cm}$
 $H = 2\text{ }\mu\text{sec/cm}$



2000 Volts, cathode at D_2

$V = 1\text{v/cm}$
 $H = 2\text{ }\mu\text{sec/cm}$



2500 Volts, cathode at D_2

$V = 1\text{v/cm}$
 $H = 2\text{ }\mu\text{sec/cm}$

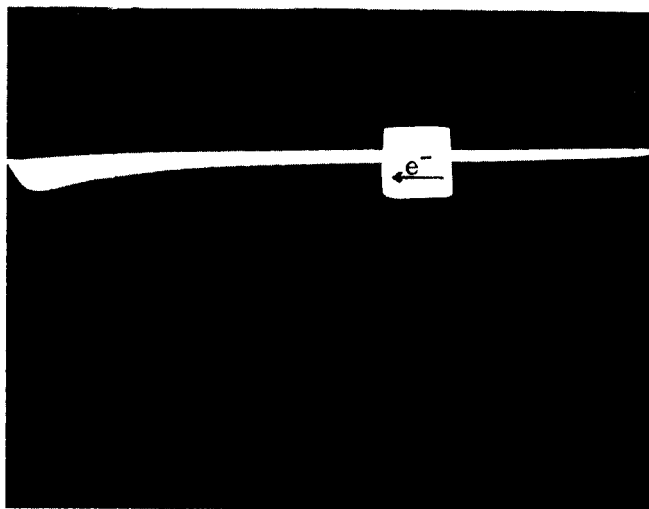
Figure 34

9.0 MULTIELECTRON PULSE INVESTIGATION

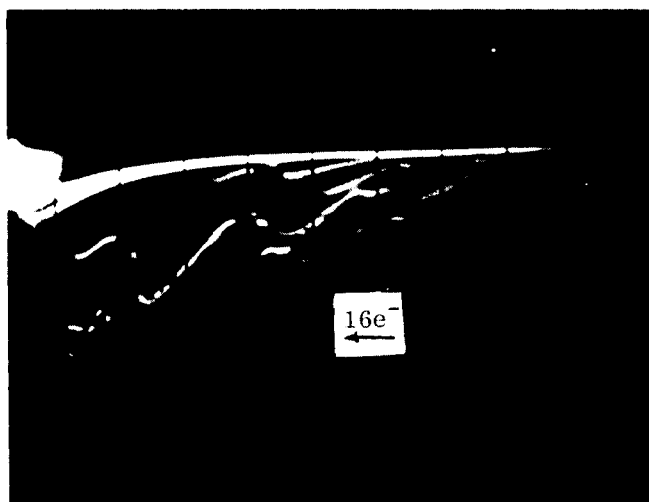
In Section 8.3 of this report, it was noted that the occurrence of multielectron pulses has been a major source of difficulty in these tubes. It appears, however, that these pulses did not occur at a high enough rate to cause serious difficulty until sapphire photocathode substrates were used. This suggests that the pulses were a function of the faceplate substrate material and not a fault inherent in the tube design. In view of this, a literature search was conducted in order to establish the properties of sapphire (Al_2O_3) as a scintillator or phosphor. It became quite obvious that Al_2O_3 did possess such capabilities when properly doped. However, specific reference was found⁸ indicating that Al_2O_3 , even in its purest form was a good scintillator with 0.5 to 0.2 times the capabilities of P-16 phosphor and that the peak of its spectral distribution is at 2750 Å, the spectral region in which the tube was to be used.

With this information in mind, an experiment was performed using radioactive Cs^{137} (2.7×10^6 γ/min.) as a means of exciting the sapphire window on one of these tubes. The results of this test are shown in Figure 35, (a) through (c). In Figure 35 (a) the dark pulses due to single thermionic electrons are shown in order to establish a reference for following photographs. In Figure 35 (b) the oscilloscope trigger was adjusted to exclude the single electron pulses and the exposure increased by 100 times. If one assumes that the average single electron produces a pulse 0.25 cm high in Figure 35 (a), then in Figure 35 (b) a pulse, with the same time constants, 3 cm, high would be equivalent to 16 electrons leaving the cathode. Inspection of Figure 35 (b) shows that the rate of these multielectron pulses is lower than for single electron pulses in Figure 35 (a), about one per second, and that they are ragged, long time-constant pulses. This would indicate that these pulses contain 16 or more individual pulses of single electron proportions which faster electronics might resolve. This has indeed been the case in the users' application, an intolerable situation where single electron counting is required. In Figure 35 (c), the conditions are the same as in Figure 35 (b) except that the Cs^{137} source has been placed on the sapphire entrance window of the tube. The pulse rate is greatly increased and the pulses appear to have the same shape as those in Figure 35 (b). From the foregoing data, it is evident that the majority of these pulses are of the order of at least 16 or more electrons, depending on their time dispersion. Figure 35 (d) is a 1-minute exposure of the dark pulses with the vertical sensitivity reduced to 1 volt/cm, so that occasionally pulses as large as 60 electrons are seen, and in Figure 35 (e) a 1-minute exposure of the dark count, at -20 degrees C, is shown on the same scale. In this photograph the multielectron pulses are seen to persist which the small pulses are reduced.

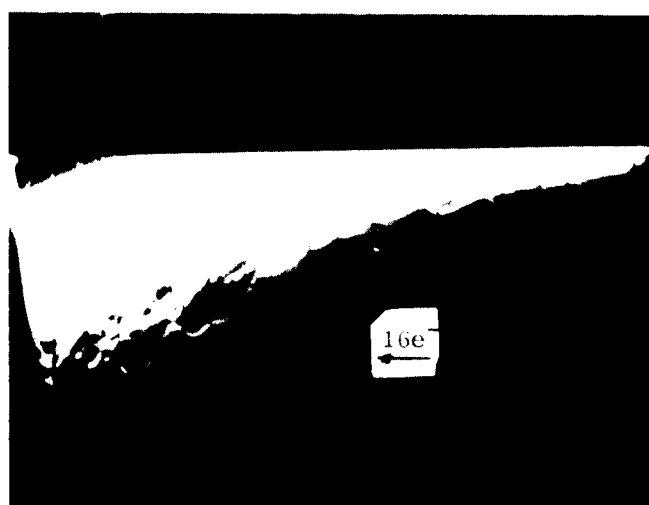
It should be noted that there is as yet no reason known for the occasional large exponential pulses as seen in Figure 35 (d), but it is assumed that these are a result of some other excitation mechanism in the sapphire window, for example, Cerenkov radiation from cosmic rays or other sources.



Exposure: 0.1 sec.
 Vert.: 0.2 v/cm
 (a) Horiz: 1 μ sec/cm



Exposure: 10 sec.
 Vert: 0.2 v/cm
 Horiz: 1 μ sec/cm
 Trigger Level Set to
 (b) Exclude e^- Pulses



Exposure: 10 sec.
 Vert: 0.2 v/cm
 Horiz: 1 μ sec/cm
 Trigger as above
 C¹³⁷ (2.7×10^6 γ /min)
 (c) Source on Photocathode.

Figure 35

All Photos are of Tube Output in the Absence
 of Luminous Flux Input to the Photocathode.



Exposure: 1 min.
 Vert.: 1 v/cm
 Horiz.: 1 μ sec/cm
 (d) Without Cs¹³⁷ Source



Exposure: 1 min.
 Vert.: 1 v/cm
 Horiz.: 1 μ sec/cm
 (e) Cathode @ -70°C

Figure 35 (Continued)

A further experiment was performed to determine the decay characteristics of the sapphire. A one millicurie Cd^{109} source was used for this purpose. Since it appeared that a more intense source was required to excite the sapphire to a level where its output would produce enough counts over a sufficient period of time for the data to be taken. A 1 Mhz totalizing counter was used in conjunction with the pulse amplifier and oscilloscope to monitor the multiplier output. The data in Figure 36 show this characteristic in terms of total counts per 0.1 minute versus time. While it is difficult to correlate this data with the relative data given in the report cited earlier, it does agree with the report in that a long time-constant decay does follow a short decay of the order of $0.1 \mu\text{sec}$, which of course, would not be detected by the technique used here.

It seems evident from the foregoing data, that sapphire is not a satisfactory choice for cathode entrance windows in tubes to be used in photon counting applications since residual radioactivity in tube parts, cosmic radiation, etc. are almost certain to produce this difficulty. Entrance windows of 9741 glass have been tried and, while it does not transmit as far into the ultraviolet as sapphire, it is a superior to sapphire, in terms of spurious pulse generation.

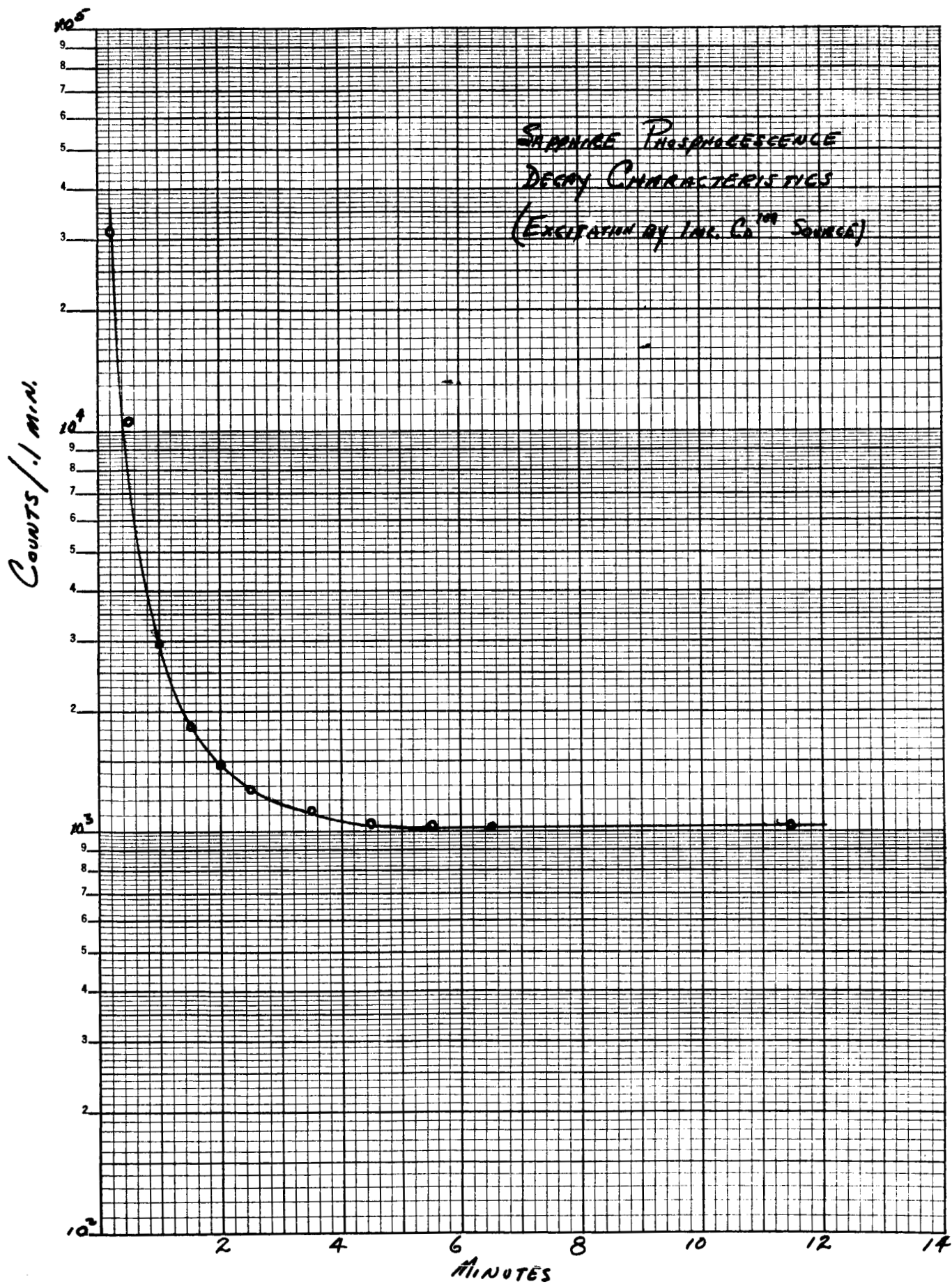


Figure 36

10.0 SECONDARY ELECTRON DEFLECTION AT DYNODE ONE

In an attempt to correct shading of the output signal of certain other multiplier phototubes, a modification of dynode one was made which seemed to hold some promise of improved multiplier statistics. This modification consisted of separating the back of dynode one from the secondary emitting surface. The expected result was the ability to deflect primary electrons by applying a negative potential to the back of dynode one, so that they would strike the front edge of the dynode. If this condition could be achieved, then the secondaries produced should see a higher dynode two collecting field and thereby decrease the probability of lost secondaries which might occur with secondaries generated towards the back of the dynode. An experimental image dissector did, indeed, show reduced signal shading when this technique was applied. It was also expected that the application of a higher potential to this electrode would result in dynode one bypassing of the primaries, which would be indicated by a sharp decrease in gain and thus output signal amplitude. The opposite effect, however, was noted. This unexpected result would lead one to conclude then that this deflecting field has a greater effect on the low energy secondaries than on the high velocity primaries. Thus, the secondaries are deflected into the dynode two collecting field before the stiffer primary beam can bypass dynode one. This then amounts to a novel method of increasing the gain of dynode one.

Since a high gain at dynode one is essential to superior single electron counting capabilities, two tubes were built incorporating this dynode one structure. Both tubes had S-20 photocathodes and 14 mil effective cathode diameters. One of these tubes was lost due to an oven failure during the photocathode formation process.

In an earlier report,⁹ a discussion was presented on the effect of varying the potential of dynode one. In view of this, the operating conditions shown in Figure 37 were established for the second tube so that the potential of the secondary emitting surface could be varied as well as that of the deflector (back of dynode one). The voltages noted on this diagram appeared to be optimum for this tube and were the voltages used when the spectra in Figure 38 were taken.

Inspection of the upper curve in Figure 38, which is signal counts plus dark counts, shows a peak to valley ratio of 2:1, undoubtedly the best distribution seen to date. The lower curve is the dark counting spectrum. This curve shows a distribution similar to signal plus dark spectrum indicating, of course, that the dark counts are thermionic electrons from the photocathode. Cooling the cathode would, no doubt, markedly reduce the dark counting rate. Figure 39 is a display, on a linear scale, of the signal plus dark count distribution for this tube.

This dynode one design has also been tried in a multiplier phototube of the type built for Lick Observatory, which was reported on last quarter. In the one tube of this type that was tested, the adjustment of the potentials applied to these two sections of dynode one failed to produce the results expected on the basis of the

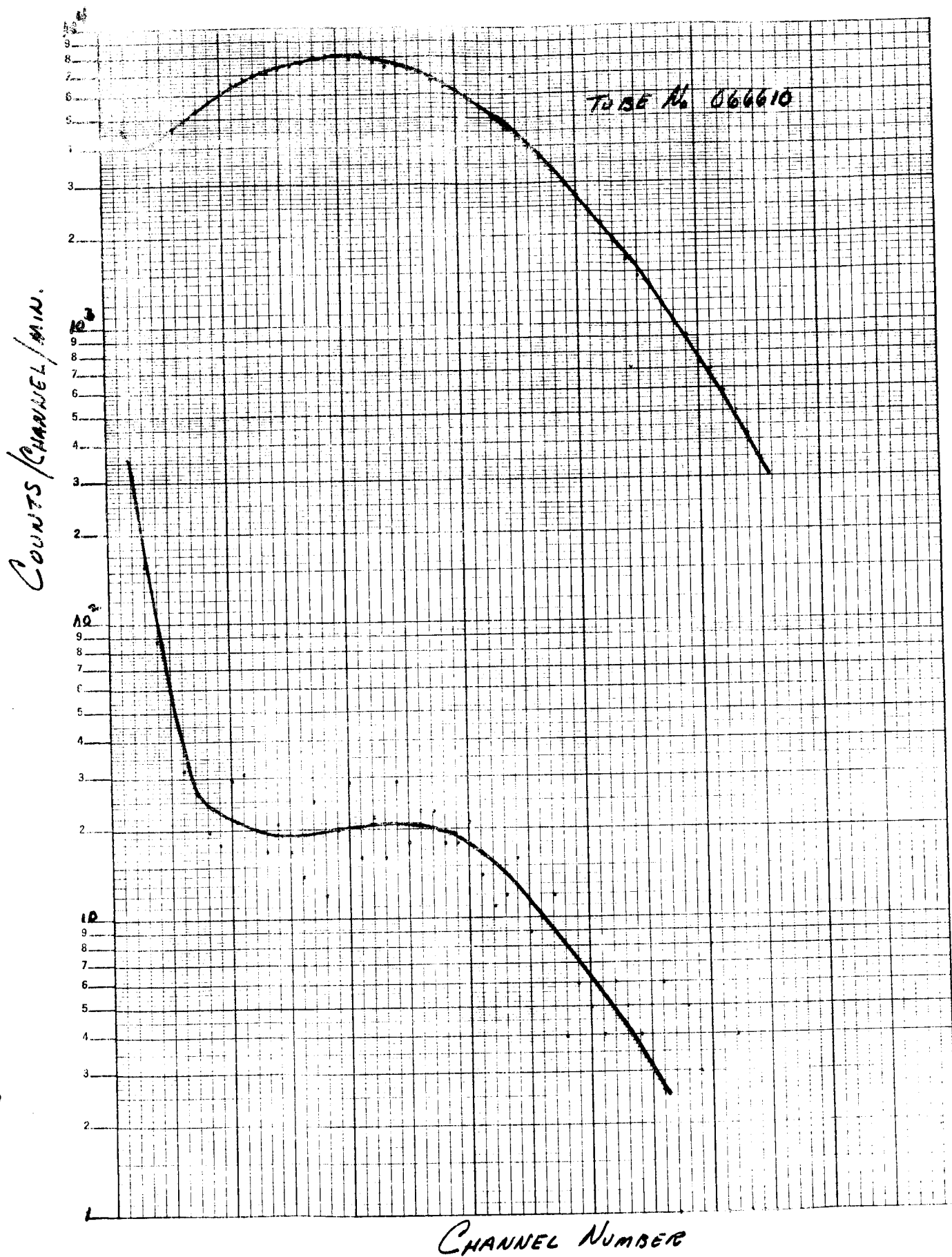


Figure 38

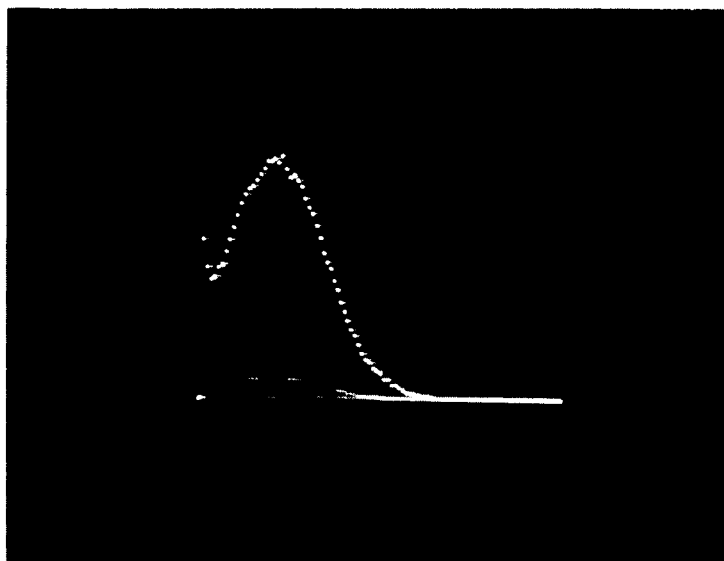


Figure 39

earlier tubes. The reason for these negative results is not presently known, but it is not unreasonable to believe that the extensive modifications made in the image section, which affect the magnification and effective cathode diameter may also have altered conditions, affecting electron collection, between dynode one and two. Further investigation of this problem is indicated to determine what corrective steps can be taken.

REFERENCES

1. ITTIL Application Note E4 (See Appendix I)
2. G. Pietri, IEEE Trans on Nuclear Science, Vol. NS-11, 1964, page 76.
3. Line Scan Dissector, USAF Contract No. AF33(615)2626.
4. J. L. Gumnick & C. D. Hollish, IRE Tr. on Nucl. Sc. NS-13, No. 3, 72 (1966).
5. University of California, Lick Observatory NASA Prime Contract 05-003-100-1 (Subcontract to ITTIL, G607170).
6. Typical Absolute Spectral Response Characteristics of Photoemissive Devices, ITTIL Wall Chart.
7. Third Quarterly Report NASw 1038 May 28, 1965.
8. Ultraviolet Phosphor Development for an Active Optical Imaging System Westinghouse Electric Corp. Aerospace Division, Baltimore, Md. for the Navy Department Bureau of Ships Electronics Division Contract No. NObs-90449 Project No. SF0070506 Task No. 10372 Final Report July 20, 1964.
9. First Quarterly Report NASw 1038 Nov. 24, 1964.

APPENDIX I

APPLICATIONS NOTE E4

COOLING CHARACTERISTICS OF ITTIL MULTIPLIER PHOTOTUBES

APPLICATIONS NOTE E4

COOLING CHARACTERISTICS OF ITTIL MULTIPLIER PHOTOTUBES

The appreciable contribution of thermionic emission from the photocathode to the anode dark current observed in some multiplier phototubes makes possible a reduction in this current and consequently in the dark noise of these tubes by cooling. Figure 1 Curve (a) shows the measured decrease in anode DC dark current, I_{DC} , in an ITTIL FW-118 multiplier phototube (S-1 type) down to photocathode temperatures of about -20 degrees C. The sharply falling dark current, approximately following a Richardson type law, substantiates the predominance of thermionic emission from the photocathode in this tube at these temperatures. A decrease of about an order of magnitude for each 10 degrees C of cooling is observed.

Figure 1 Curve (b) shows the corresponding decrease in the equivalent noise input (ENI)¹ as a function of temperature, compared to the published² ENI characteristic Curve (c) for a competitive type tube. The FW-118 starts with a lower ENI characteristic at room temperature (at least partially because of its smaller effective photocathode area) and improves about twice as fast as the competitive detector with temperature.

At anode dark current levels below about 10^{-10} amperes, reliable and significant cooling characteristics can only be observed with difficulty in many multiplier phototubes because of the erratic and nonreproducible contribution of leakage currents (in the tube stem and base and internal parts), external pickup effects, and other low current measurement difficulties. For example, a resistance of 10^{13} ohms across the surface of nominally insulating internal anode pin support (an entirely reasonable value in view of the chemically reactive cathode materials present) can contribute 10^{-10} amperes in the typical operating range of 10^3 volts. This difficulty may be further aggravated when cooling a complete tube envelope if condensation of water vapor across various tube stem and basing lead connections occurs. Noise from this latter source can be particularly troublesome if the condensation occurs between the tube stem and base, where moisture may be trapped in the base cementing process. To avoid this, ITTIL recommends the use of unbased tubes (flying lead construction) or photocathode-only cooling.

1 Defined and measured according to IRE publication No. 62IRE7. S1.

2 RCA tube manual, 7102 tube type.

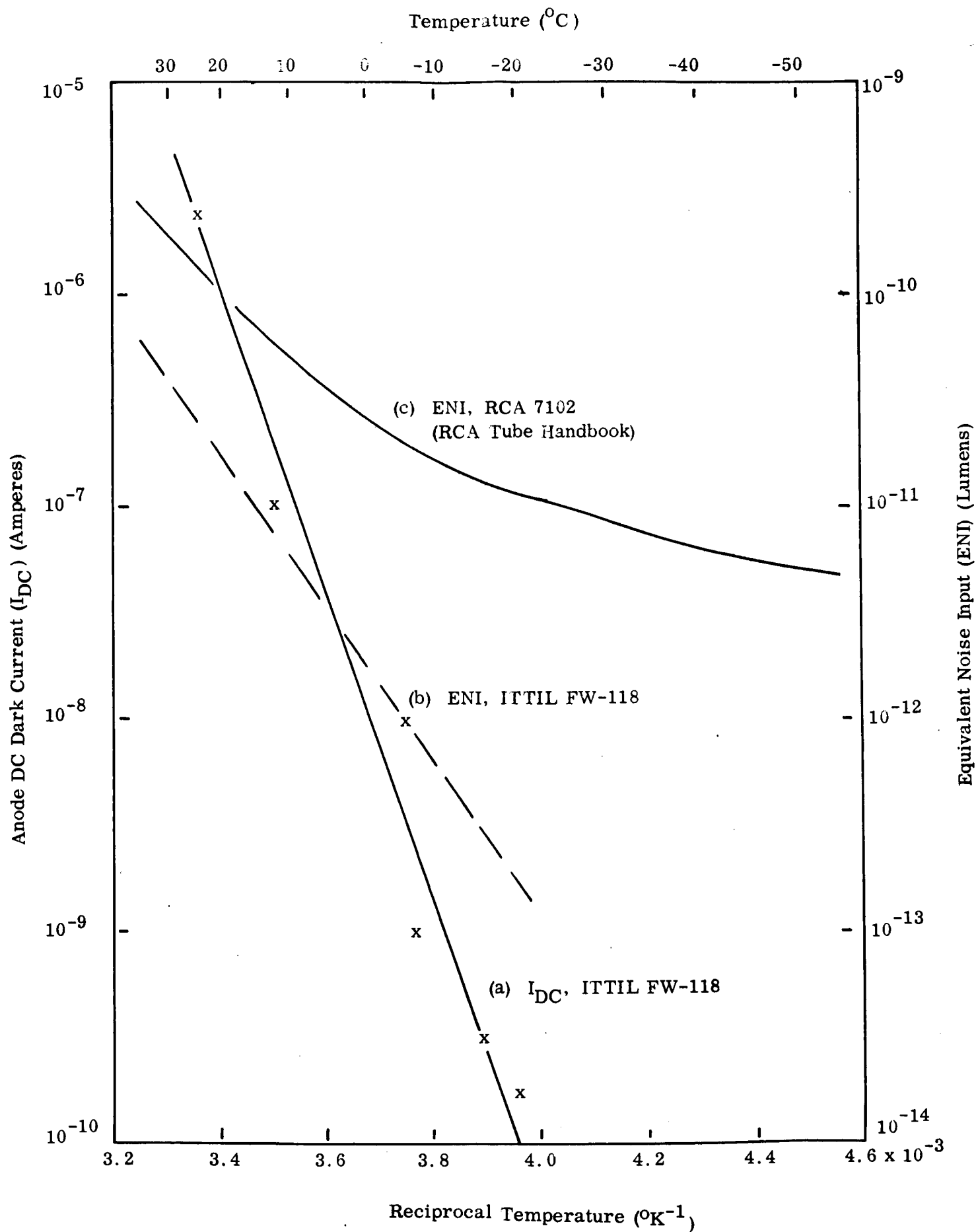


Figure 1 Anode DC Dark Current and ENI Vs Temperature for S-1 Type Multiplier Phototubes

Figure 2 shows a sketch of one type of laboratory cooling test equipment used by ITTIL. The cooled dry gas cools the tube faceplate and thus the photocathode by direct thermal contact, while the warm dry gas keeps the outer window from frosting. For field purposes, thermoelectric photocathode coolers of moderate cooling capability may be entirely adequate.

A recent and unique step taken by ITTIL to minimize internal tube leakage current and therefore improve both the room temperature and cooled dark current-dark noise characteristics, is the addition of an internal guard ring electrode surrounding the anode pin. This guard ring, when operated at quiescent DC anode potential as shown in Figure 3, bypasses surface leakage current around the anode pin and reduces the resultant minimum DC current levels to the order of 10^{-12} amperes or less. If so desired this guard ring can be voltage-driven in the more sophisticated types of feedback electrometer circuits.

For ultra-low light level detection problems, ITTIL normally recommends the use of single electron counting techniques^{3,4}. By individually counting the comparatively large pulses produced in the anode circuit of multiplier phototubes resulting from single photoelectrons from the photocathode and biasing off the smaller pulses resulting from leakage current, dynode emission, etc., maximum differentiation between signal and dark noise can be achieved.

Further cooling of ITTIL tubes below the levels shown in Figure 1 is entirely feasible, the tubes being capable of operation at dry ice temperatures and probably as low as liquid N₂ temperatures. A. T. Young of Harvard Observatory has reported⁵ a slight increase in over-all sensitivity for these tubes at dry ice and liquid N₂ temperatures combined with a reduction in dark current of at least 5 orders of magnitude at dry ice temperatures, indicating reasonably satisfactory performance, while W. A. Baum has reported⁶ dark counting rates below 10 per minute at similar temperatures. ITTIL does not recommend cooling below dry ice temperature unless the temperature cycle is slow enough (a matter of hours) and applied uniformly to the complete tube to prevent strains from developing in the tube envelope, and unless the resultant ultra-low dark thermionic emission rates are known to be desirable (in many

- 3 E. H. Eberhardt, "Multiplier Phototubes for Single Electron Counting", IEEE Tr. of Nucl. Sc., Vol. NS11, No. 2, 48, 1964.
- 4 ITTIL Research Memos 367 and 387, and Applications Note E5.
- 5 A. T. Young, Applied Optics, Vol. 2, 51 (1963).
- 6 W. A. Baum, Vol. II, Astronomical Techniques, U. of Chicago Press, 1962, page 28.

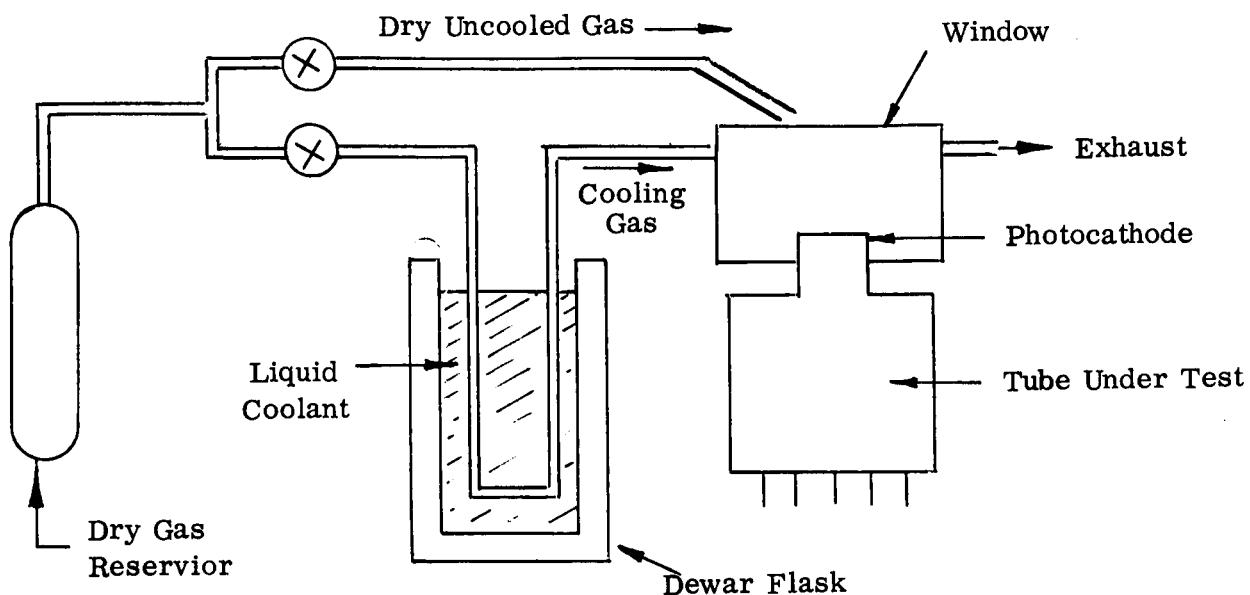


Figure 2 ITTIL Cooling Configuration

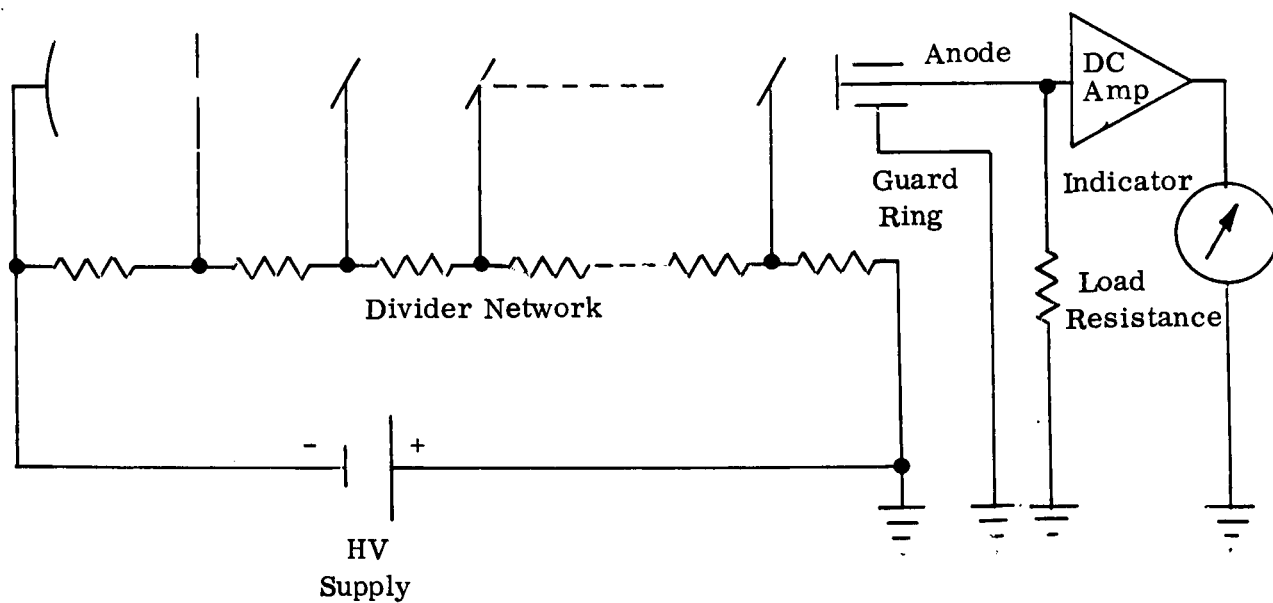


Figure 3 Typical Multiplier Phototube Circuit Using Guard Ring Electrode

applications, background light flux, present on the photocathode in the absence of the signal flux to be detected, radioactive content of the tube parts, and other dark noise sources may normally cause much more noise than photocathode thermionic emission).

The example reported by Baum in which a cooled ITTIL 16 PMI (predecessor of the present FW-118) was operated at a dark counting rate of less than 10 electrons/minute is particularly interesting. Referred to the anode circuit, under the assumption of a gain of 10^6 in the electron multiplier, this is equivalent to less than 3×10^{-14} amperes, a value well below the expected anode leakage current limits. If these 10 dark counts/minute were randomly distributed, as expected, the statistical uncertainty for a one minute observation time would have been $\sqrt{10} \cong 3$ photoelectrons, equivalent to about 13 input photons/second or a total of 750 photons in 1 minute for a peak quantum efficiency of 0.4 percent in the corresponding S-1 photocathode at 8000 Å. The ability to detect flux levels of this magnitude (approximately 3×10^{-18} watts) using single electron counting techniques with a cooled FW-118 multiplier phototube demonstrates the unique capabilities of this detector.

Cooling characteristics of S-11 and S-20 type multiplier phototubes (such as the ITTIL FW-129 and FW-130 types), are not shown in Figures 1 and 2 because of the difficulty in making reliable measurements at the dark emission rates involved. For example, a total thermionic dark count rate of only 30 electrons/second at room temperature was observed³ in one sample ITTIL FW-129 tube. This magnitude is believed to be typical of present S-11 and S-20 tubes. Based on tentative experimental measurements it is believed that these thermionic emission dark current count rates will also fall rapidly with cooling.